

Development of gold particles at varying precursor concentration

Mubarak Ali ^{a, *} and I –Nan Lin ^b

^a Department of Physics, COMSATS University Islamabad, Park Road, Islamabad-45550, Pakistan, *E-mail: mubarak74@mail.com, mubarak74@comsats.edu.pk

^b Department of Physics, Tamkang University, Tamsui, New Taipei City 25137, Taiwan

Abstract –Coalescence of tiny-sized particles into large-sized particles has been an overlooked phenomenon for a long time. This study focuses on the development of gold particles under varying precursor concentration in a custom-built setup. Under the tuned ratio of bipolar pulse OFF to ON time, tiny particles of different size and shape develop depending on the amount of gold precursor. Nano-energy of pulse packets bind gold atoms into own shape when they morph in compact monolayer assembly at solution surface. Between precursor concentration 0.07 mM to 0.90 mM, developing of tiny particles are both in triangular-shape and non-triangular-shape. Tiny particles of triangular-shape develop in a large number at precursor concentration 0.30 mM and 0.60 mM. Prior to develop anisotropic particles, joined triangular-shape tiny particles separated into two triangle-shaped tiny particles under the application of force in surface-format. Prior to assemble, atoms of one-dimensional arrays of such tiny particles elongate to modify for structures of smooth elements. Structures of smooth elements assemble to develop different anisotropic particles at the point where exerting force in surface-format is ended. When the precursor concentration was 0.05 mM and 1.20 mM, tiny-sized particles do not develop in a triangular-shape and their packing under the mixed-behavior of forces is largely developed into particles of distorted shapes. Anisotropic particles show different structure than the distorted particles. At 50 sccm Argon flow rate, particles get developed in the same shapes as for the case of 100 sccm Argon flow rate but colors of their solutions indicate a bit different elongation rate of atoms forming structures of smooth elements. This study clarifies the necessary concentration of gold precursor to develop particles of different size and shape.

Keywords: Precursor concentration; Nano-energy; Tiny-shaped particles; One-dimensional particles; Multi-dimensional particles; Distorted particles

1. Introduction

Developing the different structures of colloidal matter under a certain processing strategy may be the origin of a persuaded phenomenon, where their particles of controlled-shape can be the strong candidates. This is because of a great challenge to develop anisotropic particles. To assemble tiny-sized particles precisely is a goal for developing advanced functional materials. Metallic colloids having different shapes under different processing conditions may reveal the unexplored factors of their developments. When tiny-sized particle is developed by atom-to-atom amalgamation, attained-dynamics of atoms can be the sole cause. To regulate the structure of tiny-sized particles developing shape of large-sized particle, a tailored amount of energy is found to be another cause. Electron-dynamics in amalgamated atoms of certain nature may regulate the structure and, so, morphology of their bigger size. However, this (electron-dynamics) can't be the case when those atoms bind into a tiny particle under certain transitional-state. Here, prior to binding of those atoms (under certain protocol of energy), they have been amalgamated for favorably attained-dynamics and by morphing the monolayer assembly at flat solution surface. It is expected that under variable concentration of gold precursor, in an appropriate range, it may result into depict the overall picture of size, shape and structure of particles.

Here, transitional-state of an atom and electron-dynamics of an atom are two different behaviors; in the first case, electrons should be mainly recognized to deal/undertake infinitesimal displacements (under varying their force-energy in the atom) when remaining within their occupied-states (clamped-energy-knots) and, in the latter case, electrons should be mainly recognized to leave their occupied-states (for suitable force or energy) prior to re-instate states (in the outer ring of atom).

Several approaches have been explored in the literature to synthesize colloidal tiny-sized particles and large-sized particles where citrate reduction method is one of the most widely adopted procedures [1]. Development of large-sized particles on likely coalescence of tiny-sized particles has been the subject of several studies [2-12]. Metal

clusters behave like simple chemical compounds and could find applications in catalysis, sensors and molecular electronics [2]. Discrete features of nanocrystals and their tendency to extend into superlattices suggest ways and means for the design and fabrication of advanced materials with controlled characteristics [3]. An ordered array of nanoparticles instead of agglomeration might present new properties different from the individual particles [4]. Coalescence of nanocrystals into extended shapes has been appeared to be a realistic goal [5]. Self-assembly means to design specific structure, which cannot be achieved alternatively [6]. Potential long-term use of nanoparticle technology is to develop small electronic devices [7]. Assembling of nanoparticles may be an initial effort towards the selective positioning and patterning at large area [8]. Organization of nanometer size building blocks into specific structures to construct functional materials and devices is one of the current challenges [9]. On assembling nanocrystals into useful structures, 'atoms and molecules' will be treated as materials of tomorrow [10]. Precise control on the assemblies of nanoparticles enables the synthesis of complex shapes and will provide pathways to fabricate new materials and devices [11]. Coalescing nanocrystals into long-range crystals allows one to develop materials with endless selections [12]. Surface plasmon absorption is workable for small-sized anisotropic particles, but it has remained a challenging task to take benefit of the phenomenon at macroscopic level [13].

On trapping mobile electrons, tiny particles of gold collectively oscillate [14]. The existing mechanistic interpretations are insufficient to explain several observations [15]. The rate of reactant addition/reduction can be estimated to produce subsequent specific shaped particles in high yields [15]. Locating the specific mode of excitation of surface plasmon in metallic nanocrystals will bring intense consequences on the research fields [16]. More work is required to develop an in-depth understanding of metallic colloids [17].

Attempts have also been made to synthesize different geometric anisotropic particles and distorted particles in different employed plasma solution processes [18-25] where four main strategies have remained in utilization i.e., DC plasma discharge in contact with the liquid, DC glow discharge plasma in contact with liquid, pulse plasma discharge inside the liquid, and gas-liquid interface discharge. Quite a few reaction

mechanisms proposed by different groups are to be the most probable underlying mechanisms such as plasma electrons [20], hydrogen radicals in liquid [22], aqueous electrons [21] and hydrogen peroxide [18, 19]. Gold nanoplates and nanorods have been synthesized at the surface of solution while sphere-shaped particles inside the solution [22]. Again, probing matter at a length scale comparable to the subwavelength of light can deliver phenomenal optical properties [26, 27] and different phase-controlled syntheses give an improved catalytic activity of metallic nanostructures as compared to bulk ones [28, 29]. Different tiny-sized particles of gold having different attained dynamics of their amalgamation were discussed [30]. Splitting Argon atoms had switched medium of propagating photons to medium of travelling photons under increasing wavelength, where light-glow was observed on reaching wavelength of those photons in the visible range [31]. Photons having characteristic (wavelength) of current keep continuity in propagating their forcing energy in the inter-state electron gaps [32], thus, they propagate between electron states to work as photonic current [31]. The amalgamated atoms bind under generated energy of the targeted atom while executing confined inter-state electron-dynamics [33]. A separate study has discussed the mechanism of development of a triangular-shape gold tiny particle and modification of atoms of one-dimensional arrays into structures of smooth elements [34]. Carbon atoms of different states bind into tiny grains, grains or crystallites depending on the localized process conditions [35, 36]. Different tiny-sized particles and large-sized particles while processing gold precursor, silver precursor and their binary composition were discussed where processing of gold solution resulted into anisotropic particles [37]. Morphology-structure of gold particles controlled under the varying conditions of the process while employing the pulse-based electron-photon-solution interface process [38]. While considering formation of tiny particles and their extended shapes, origin of physics and chemistry of materials was discussed [39]. Gold particles of unprecedented features developed while setting the optimized condition of the process [40]. The origin of different natured atoms belonging to gas and solid states along with transitional behaviors was discussed [41]. Depending on the nature of atoms of tiny-sized particles, their use can be defective for a certain nanomedicine application [42].

Present study describes how to develop gold tiny-sized particles and their different shape large-sized particles while varying the concentration of gold precursor. We briefly discussed the role of varying precursor concentration under fixed process parameters while developing particles of different shapes in custom-built pulse-based electron-photon-solution interface process.

2. Experimental details

Solid powder of HAuCl_4 was purchased from Alfa Aesar to obtain the aqueous solution of different molar concentrations. Briefly, aqueous solution of one-gram $\text{HAuCl}_4 \cdot 3\text{H}_2\text{O}$ and ~ 100 ml DI water was prepared in a glass bottle. This was followed by the preparation of several different molar concentrations by dissolving various amounts of precursor in DI water. The total quantity of the solution for each experiment was ~ 100 ml. Schematic of the setup is shown in Figure 1.

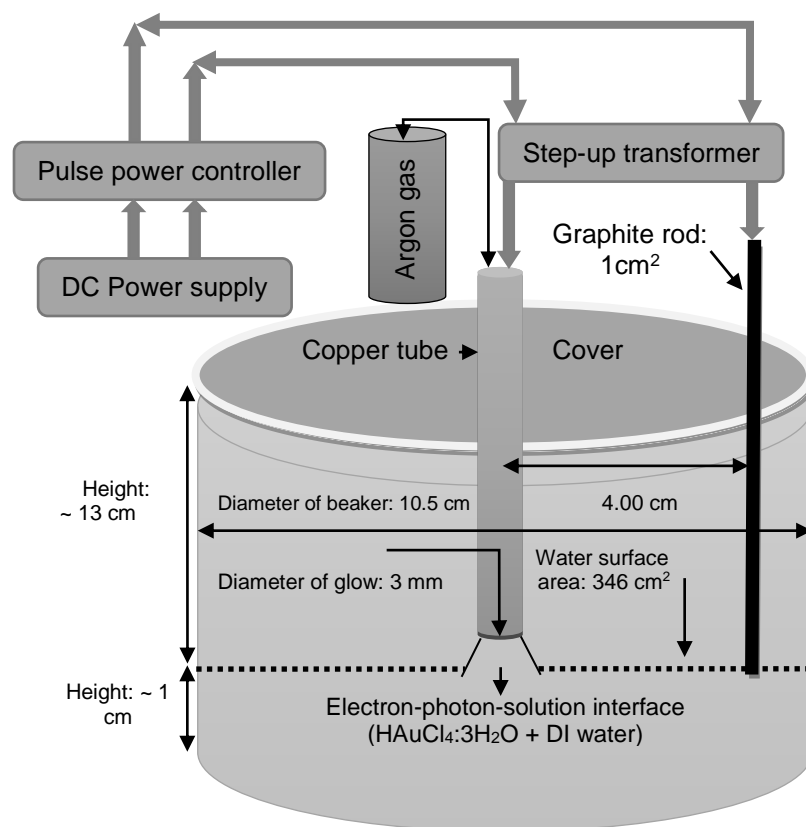


Figure 1: Schematic of pulse-based electron-photon-solution interface process

A copper capillary (electron-photon source) with internal diameter ~ 3 mm (thickness: ~ 1.5 mm) was used to maintain the flow of Argon gas. At the bottom of tube, atoms of flowing Argon gas splitted by propagating photons having wavelength (characteristic) of current. A graphite rod (energy source) with a width of ~ 1 cm was immersed into the solution known as anode. The distance between copper capillary bottom and solution surface was ~ 5 mm and was kept constant in all experiments. Distance between graphite rod and copper capillary was set ~ 4 cm in each experiment. Layout of air-solution interface and electron-photon-solution interface is shown elsewhere [30].

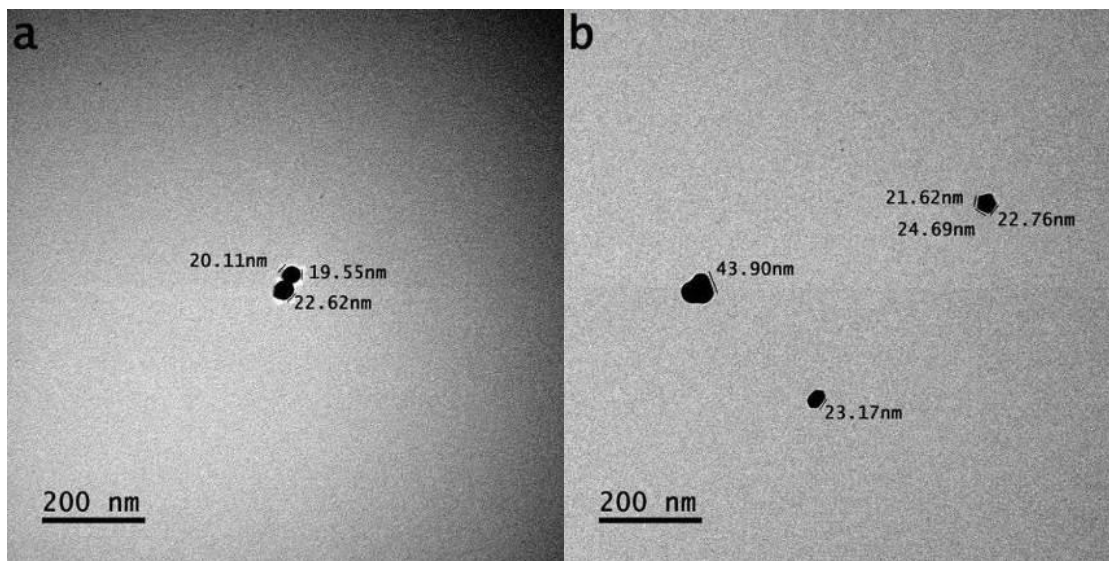
Bipolar pulse of fixed ON/OFF time was being controlled by the pulse DC power controller (SPIK2000A-20, MELEC GmbH; Germany). Input DC power was provided by SPIK2000A-20. Symmetric-bipolar mode of pulse power controller was employed, and equal time periods of pulses was set; t_{on} (+/-) = 10 μ sec and t_{off} (+/-) = 10 μ sec. The input power slightly fluctuated, initially. Fluctuation of input power was maximum at the start of the process, dropped to nearly half in a second and remained almost stable in the remaining period where the splitting of inert gas atoms was controlled automatic. The stable value of the voltage was 32 volts where current reading was noted 1.3 amp. The power was enhanced ~ 40 times under the application of step-up transformer. The variation in power was noticed ~ 1 % in the execution of new experiment for each concentration of precursor.

Temperature of the solution was recorded with laser-controlled temperature meter (CENTER, 350 Series). In each experiment, temperature was measured at the start ($\sim 20^\circ\text{C}$), middle ($\sim 27^\circ\text{C}$) and at the end ($\sim 37^\circ\text{C}$) of process with $\pm 1^\circ\text{C}$ accuracy. Different molar concentrations were prepared (~ 0.05 mM, ~ 0.10 mM, ~ 0.30 mM, ~ 0.60 mM, ~ 0.90 mM and ~ 1.20 mM), where duration of the process was set 10 minutes in each experiment. Total Argon gas flow rate was determined to be 100 sccm, which was maintained through mass flow controller. Different molar concentrations were also prepared (~ 0.07 mM, ~ 0.10 mM, ~ 0.30 mM and ~ 0.60 mM) at 50 sccm Argon gas flow rate, where other parameters were kept the same as for the case of processing solutions at 100 sccm Argon gas flow rate.

Copper grid covered by carbon film was used and samples were prepared by dip-casting. Samples were placed into Photoplate degasser (JEOL EM-DSC30) for ~ 24 hours to eliminate moisture. Bright field transmission microscope images, selected area photons reflection (SAPR) patterns (known as SAED patterns) and high-resolution transmission microscope images were taken under the application of microscope known as HR-TEM (JEOL JEM2100F) while operating at 200 kV.

3. Results and discussion

Layout of the pulse-based electron-photon-solution interface process is shown in Figure 1 by which nanoparticles and particles developed for different concentration of gold precursor, where coalescences of tiny-sized particles occur. At precursor concentration 0.05 mM, sphere-shaped and less-distorted nanoparticles were developed as shown by different bright field transmission microscope images (a-d) in Figures 2. The average size of nanoparticle is between 20 to 25 nm. This indicates that tiny-sized particles developed in the formation of such nanoparticles only constituted few gold atoms.



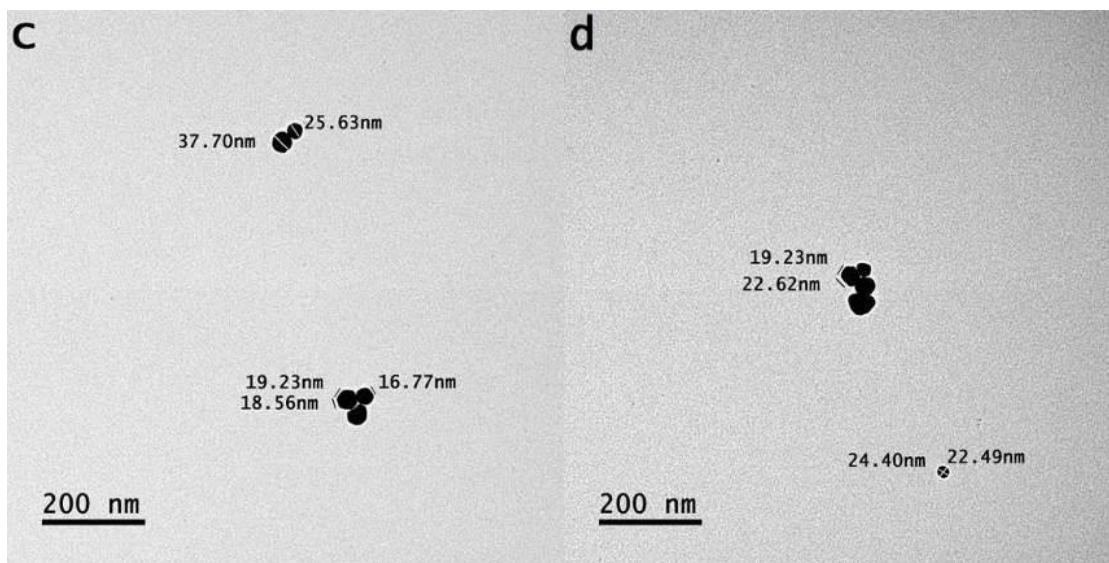
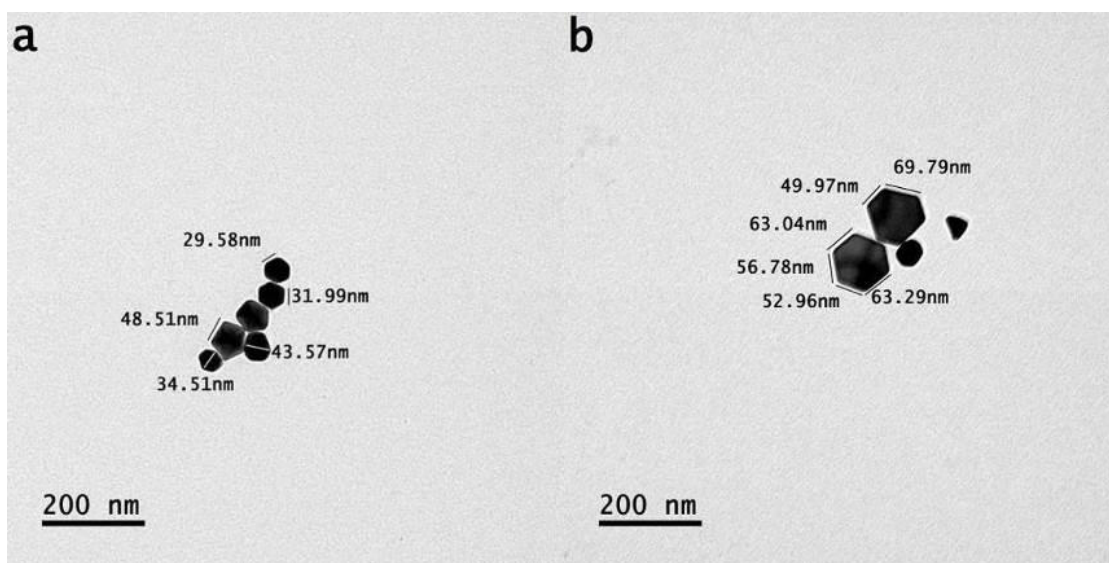


Figure 2: (a-d) bright field transmission microscope images of nanoparticles showing various less-distorted shapes; precursor concentration 0.05 mM and Argon gas flow rate 100 sccm

On increasing the precursor concentration from 0.05 mM to 0.10 mM, the average size of particles also became large where many of them developed in geometric anisotropic shapes as shown by bright field transmission microscope images in Figure 3 (a-c). The number of amalgamating atoms per unit area has increased. So, the size of tiny particle is also increased. Here, tiny particles also get developed in the geometric triangular-shape in a quite large number. So, their assembling under the certain mechanism also gets developed into nanoparticles of anisotropic shapes.



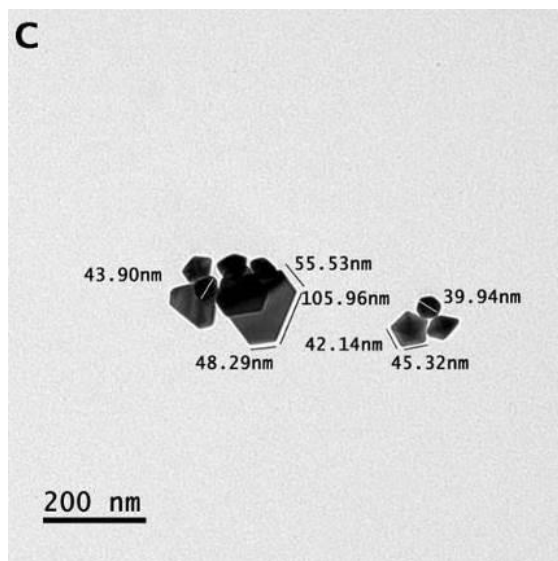


Figure 3: Bright field transmission microscope images of nanoparticles showing both geometric anisotropic and distorted shapes; precursor concentration 0.10 mM and Argon flow rate 100 sccm

At precursor concentration 0.30 mM, the average size of particles having different anisotropic shapes gets increased further. The bright field transmission microscope images of triangle-, hexagon-, isosceles trapezoid-, rhombus-, pentagon-, rod- and bar-shaped particles are shown in Figure 4 (a) & (b). The particles show high aspect ratios and their increase in size is related to increase in size of tiny particles. As the size of tiny particles having geometric triangular-shape is increased further. So, assembling gets developed for both nanoparticles and particles.

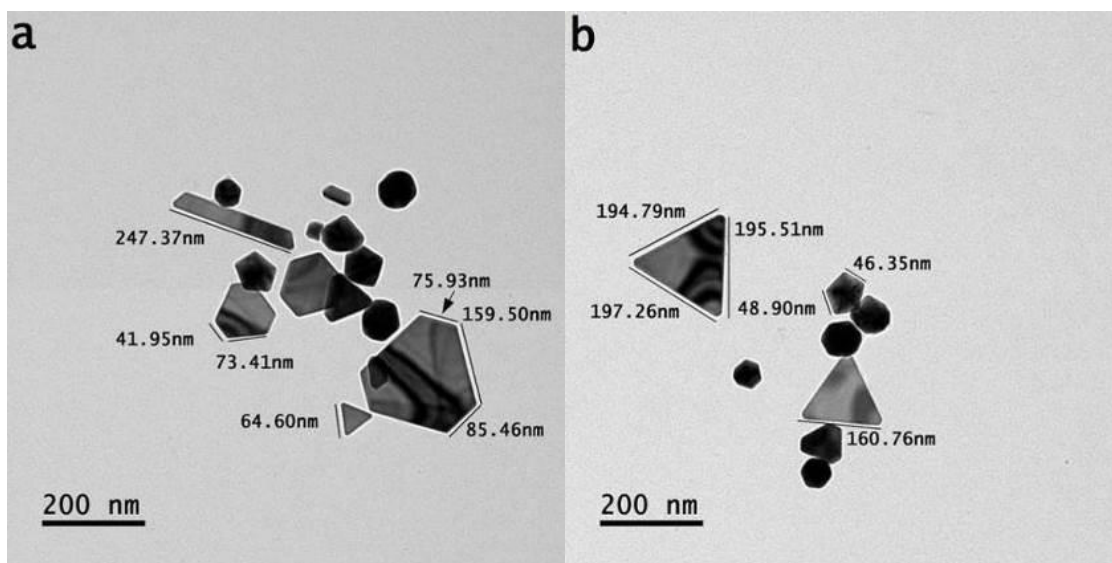
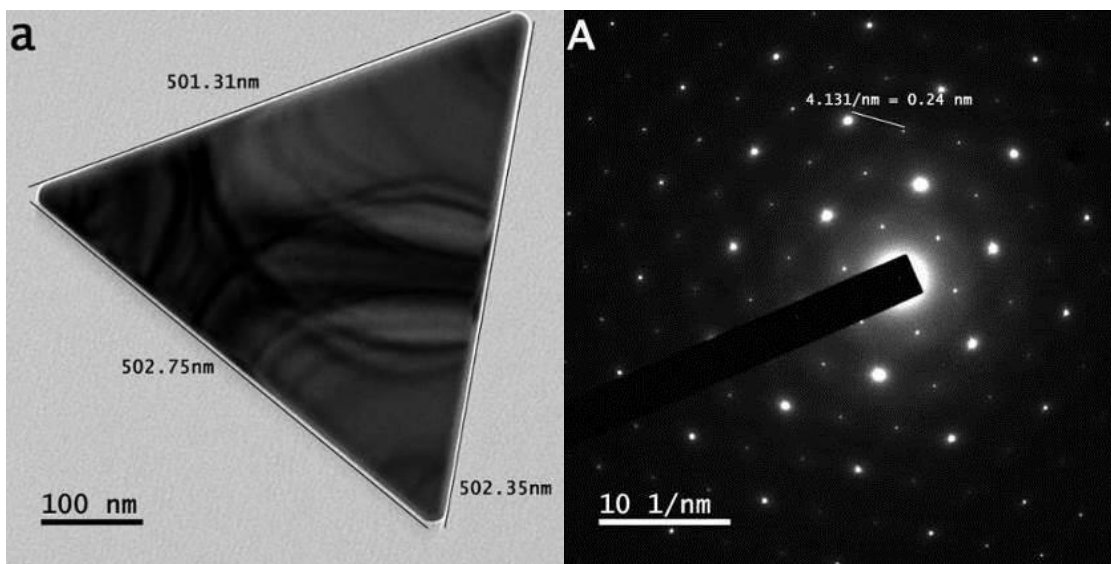
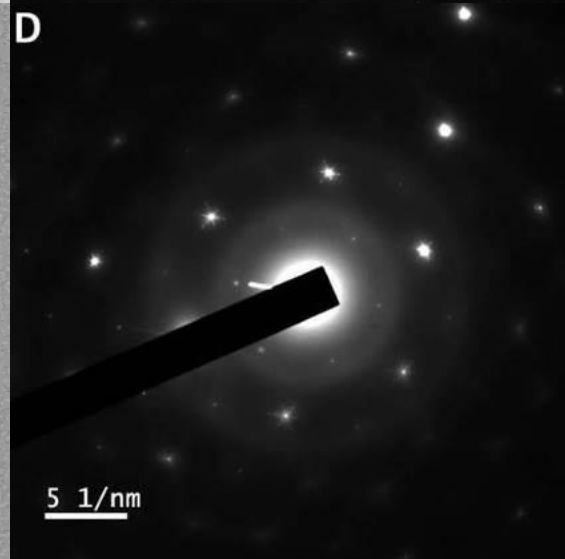
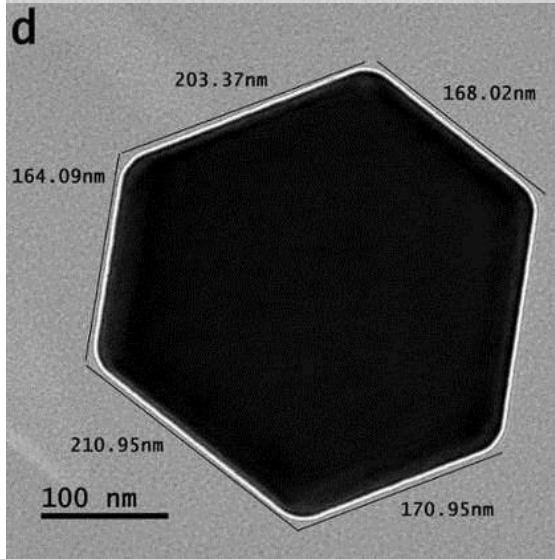
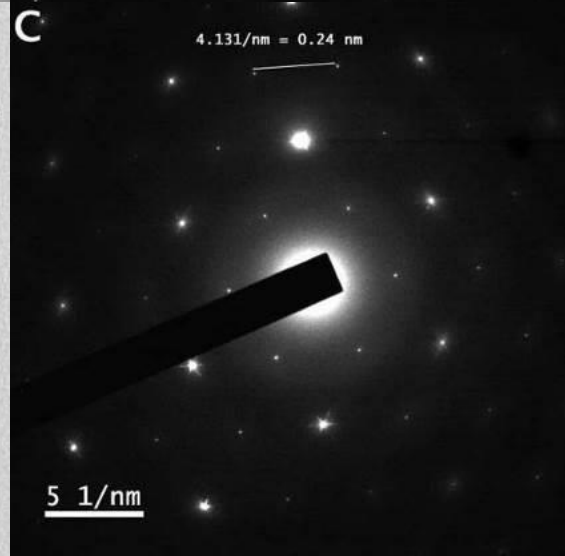
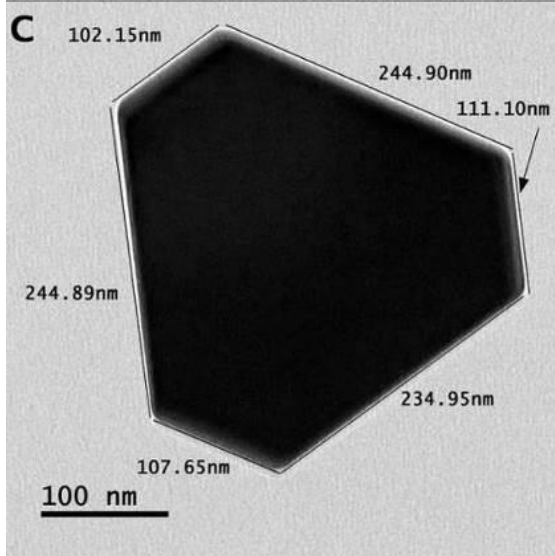
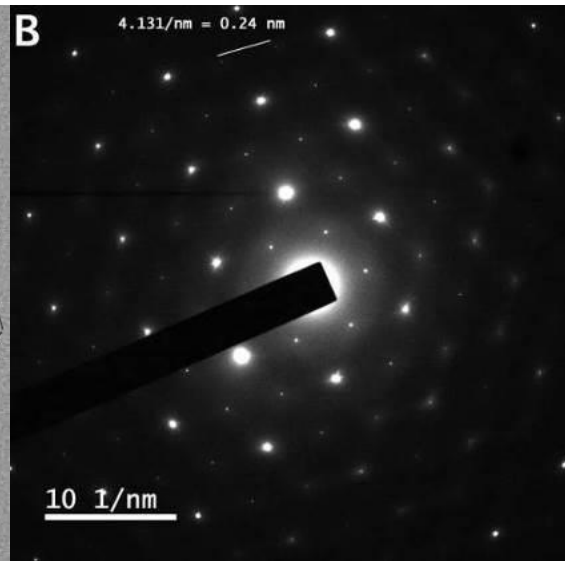
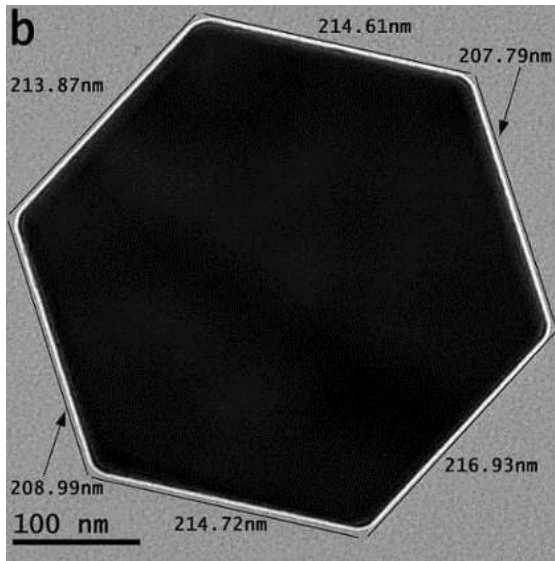
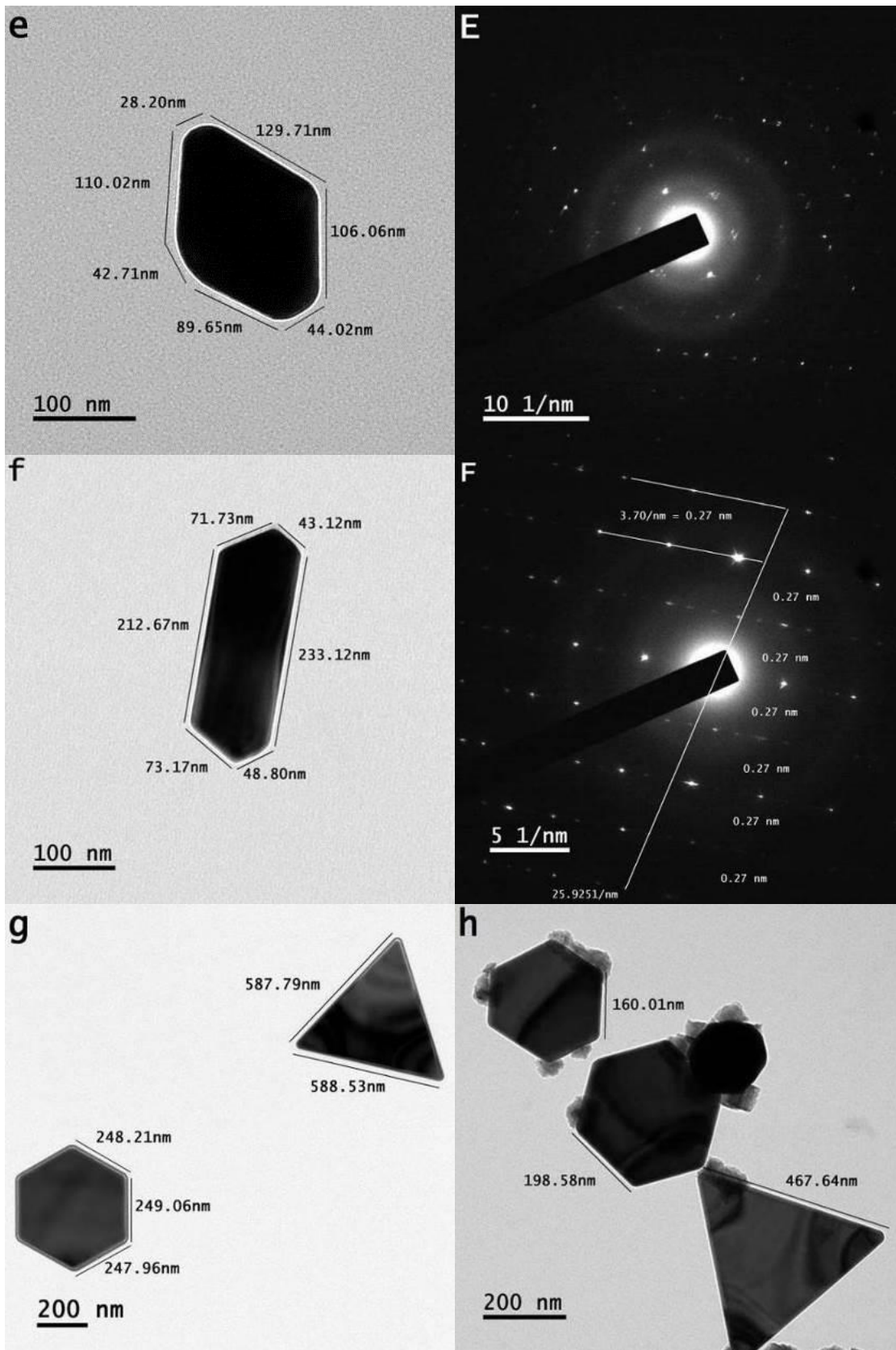


Figure 4: (a) & (b) bright field transmission microscope images of nanoparticles/particles developed in various geometric anisotropic shapes and distorted shapes; precursor concentration 0.30 mM and Argon gas flow rate 100 sccm

Several high aspect ratio shapes are shown by bright field transmission microscope images in Figures 5 (a-f) along with their SAPR patterns in Figure 5 (A-F); each image shows a unique geometric anisotropic shape of the particle along with SAPR pattern. SAPR patterns of geometric anisotropic particles indicate one-dimensional shapes in the case of bar- and rod-shaped particles, whereas, multi-dimensional shapes in the case of triangle- and hexagon-shaped particles. In Figure 5 (g), difference in the sides' length of particles (triangle- and hexagon-shaped particles) is within the margin of an atom or few atoms. This indicates that same size tiny particles were packed for them. These particles get developed under the equal rate of assembling (packing) tiny-shaped particles to all sides. In some cases, the particles bind *via* their sides (Figure 5h) and, in other cases, they are overlaid by one another (Figure 5i). But they are related to distorted particles.







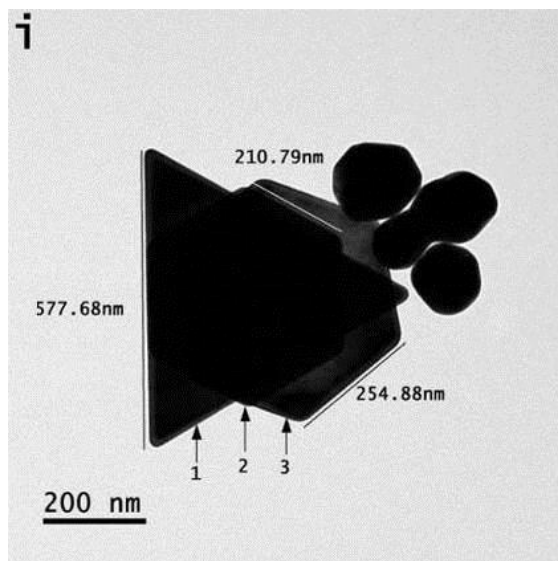
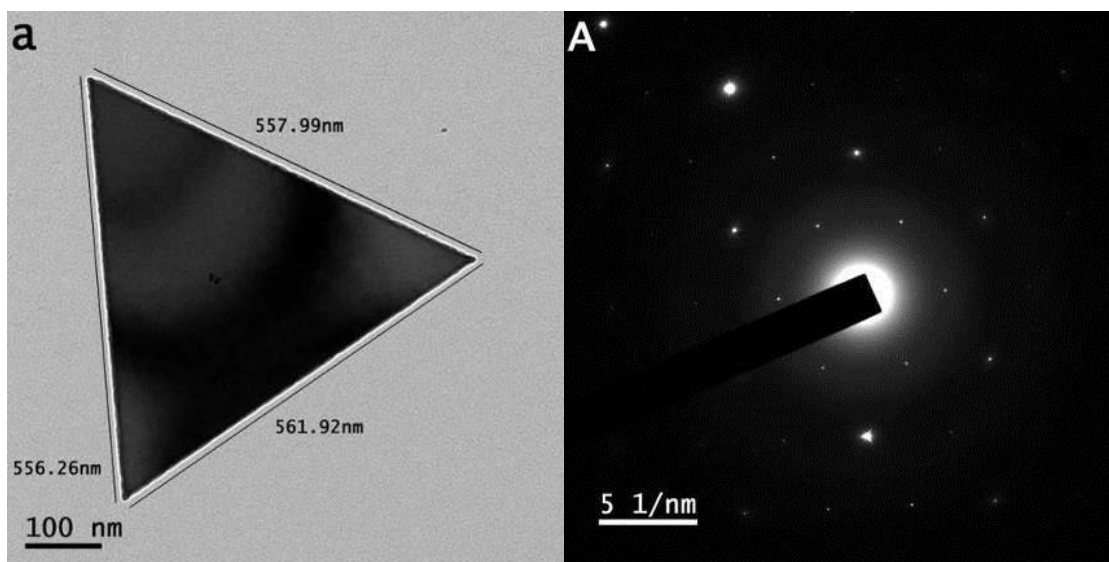
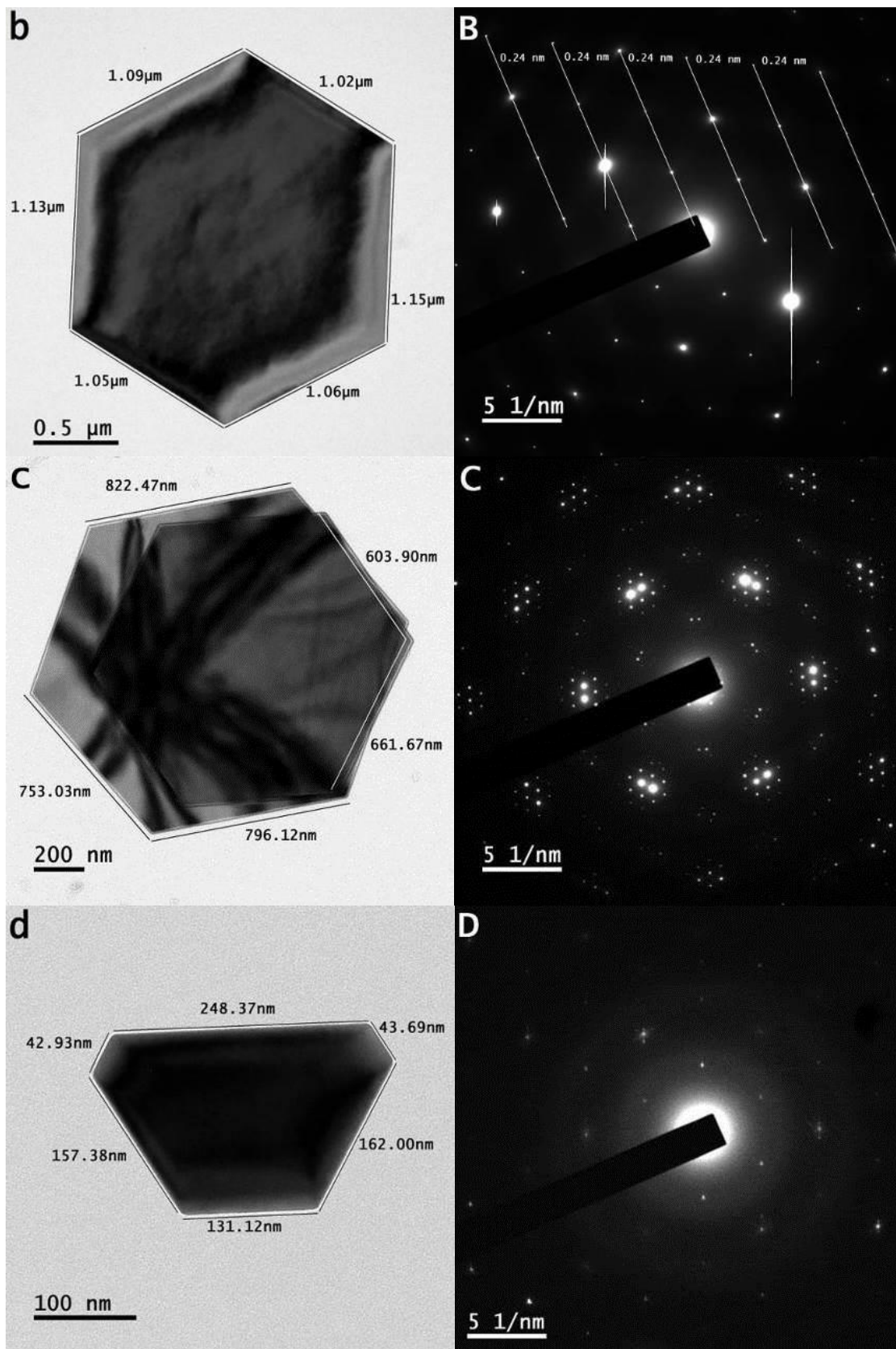


Figure 5: (a-i) bright field transmission microscope images of particles showing both geometric anisotropic shapes and distorted shapes along with SAPR patterns (A-F); precursor concentration 0.60 mM and Argon gas flow rate 100 sccm

For precursor concentration 0.90 mM, particles of different geometric anisotropic shapes are shown by bright field transmission microscope images in Figure 6 (a-h), which show the similar features as in the case of particles (and nanoparticles) developed at precursor concentrations 0.10 mM, 0.30 mM and 0.60 mM. However, particles developed at 0.90 mM possess a low aspect ratio also. More particles get developed in distorted shapes at precursor concentration 0.90 mM.





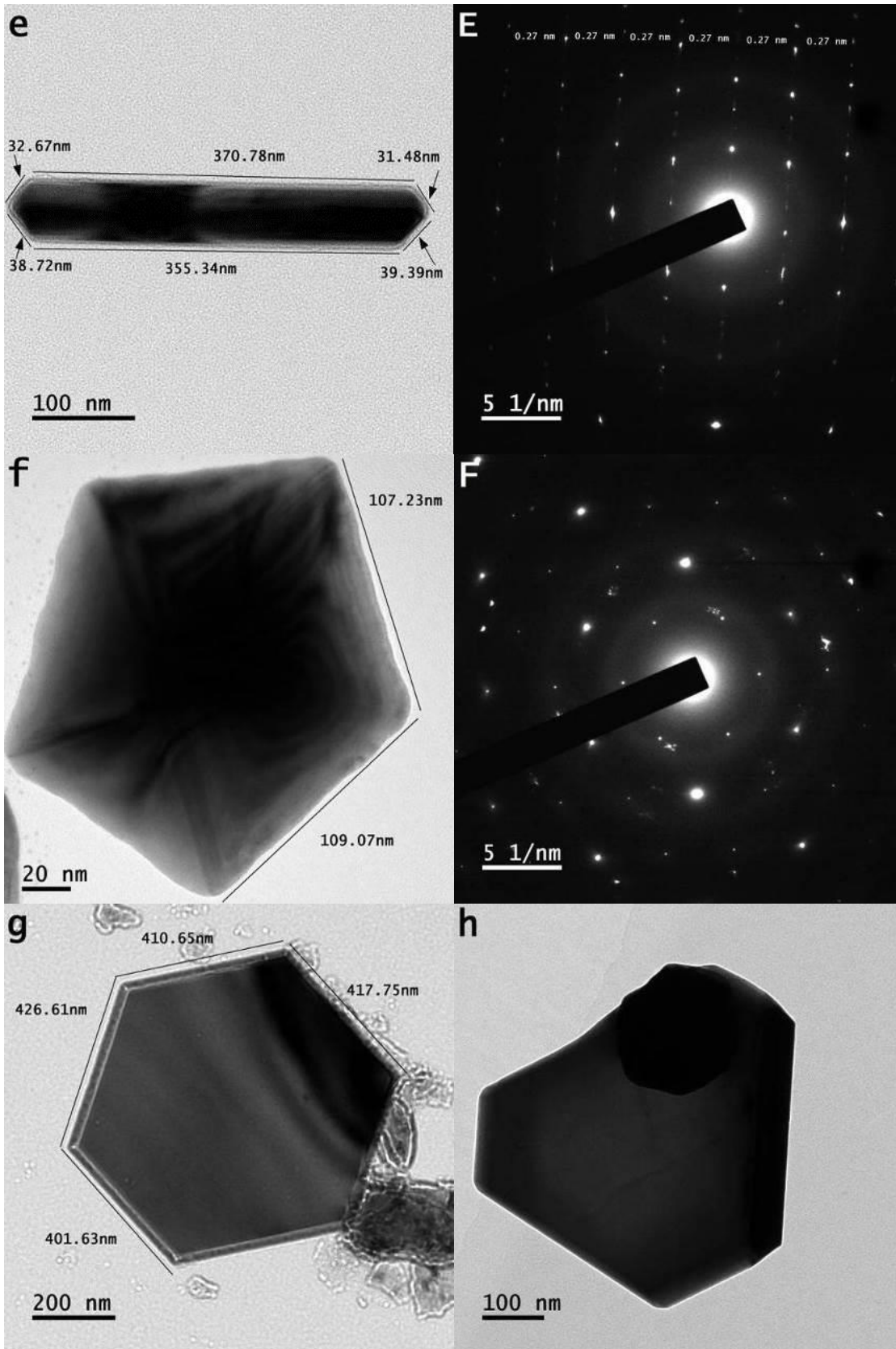
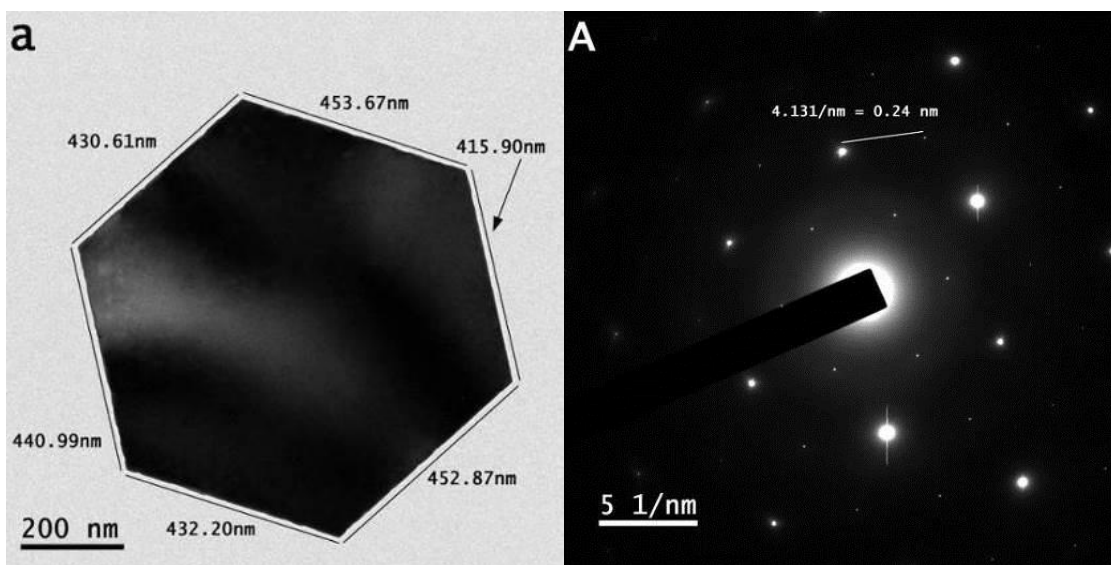
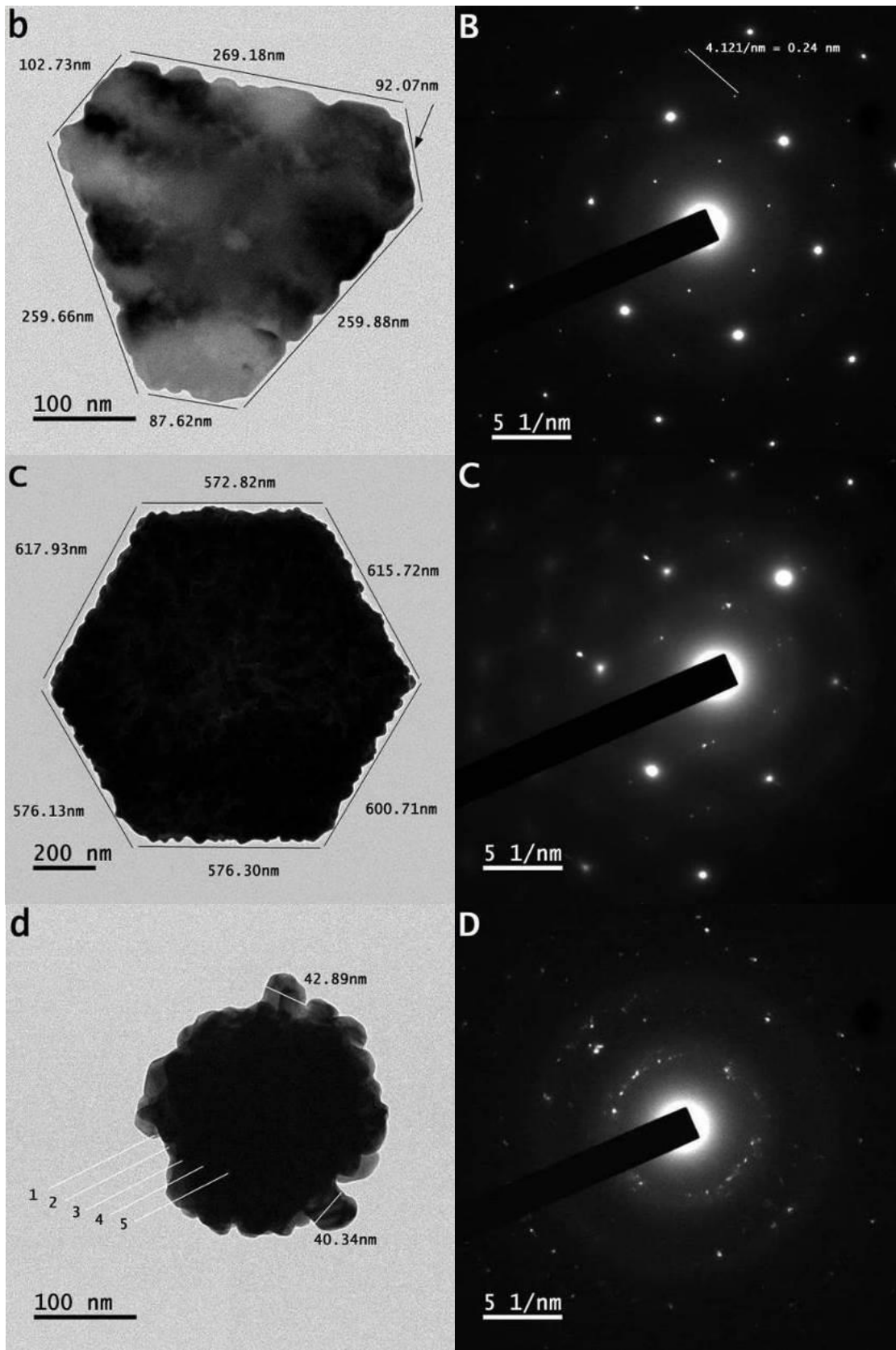


Figure 6: Bright field microscope images of particles showing both anisotropic and distorted shapes along with SAPR patterns (A-F); precursor concentration 0.90 mM and Argon flow rate 100 sccm

At 1.20 mM, very large size tiny particles get packed under the influence of forces in mixed-behaviors which resulted into develop highly-distorted particles as shown by various bright field transmission microscope images in Figure 7 (b-j). Only the particle of hexagonal-shape shows anisotropy as shown in Figure 7 (a). SAPR patterns of different shape particles show irregular structure. The spotted spots of photons in the patterns reflected at the surface of particles (shown in Figures 7a & 7b) covering few elongated atoms indicate uniform structural features (shown in Figure 7A and Figure 7B) as the chosen area of each pattern is only few square nanometers. However, the elongation of atoms is not uniform in the case of distorted particles as shown in Figures 7 (c) and 7 (d) where their structural features are evident that distribution of spotted intensity of reflected photons at selected area in Figure 7 (C) and Figure 7 (D) is not in the repeated order. The very large-sized packed tiny particles do not indicate the orientation-based (uniform) elongation of their atoms as the shape of developed particle is distorted as shown in Figure 7 (d). Distorted particle shape-like flower is shown in Figure 7 (e) and several particles of identical features are shown in Figure 7 (i). In Figure 7 (e), an average size of tiny particle is 50 nm, which is the cause of development of highly-distorted particles where they have the highly-disordered structure.





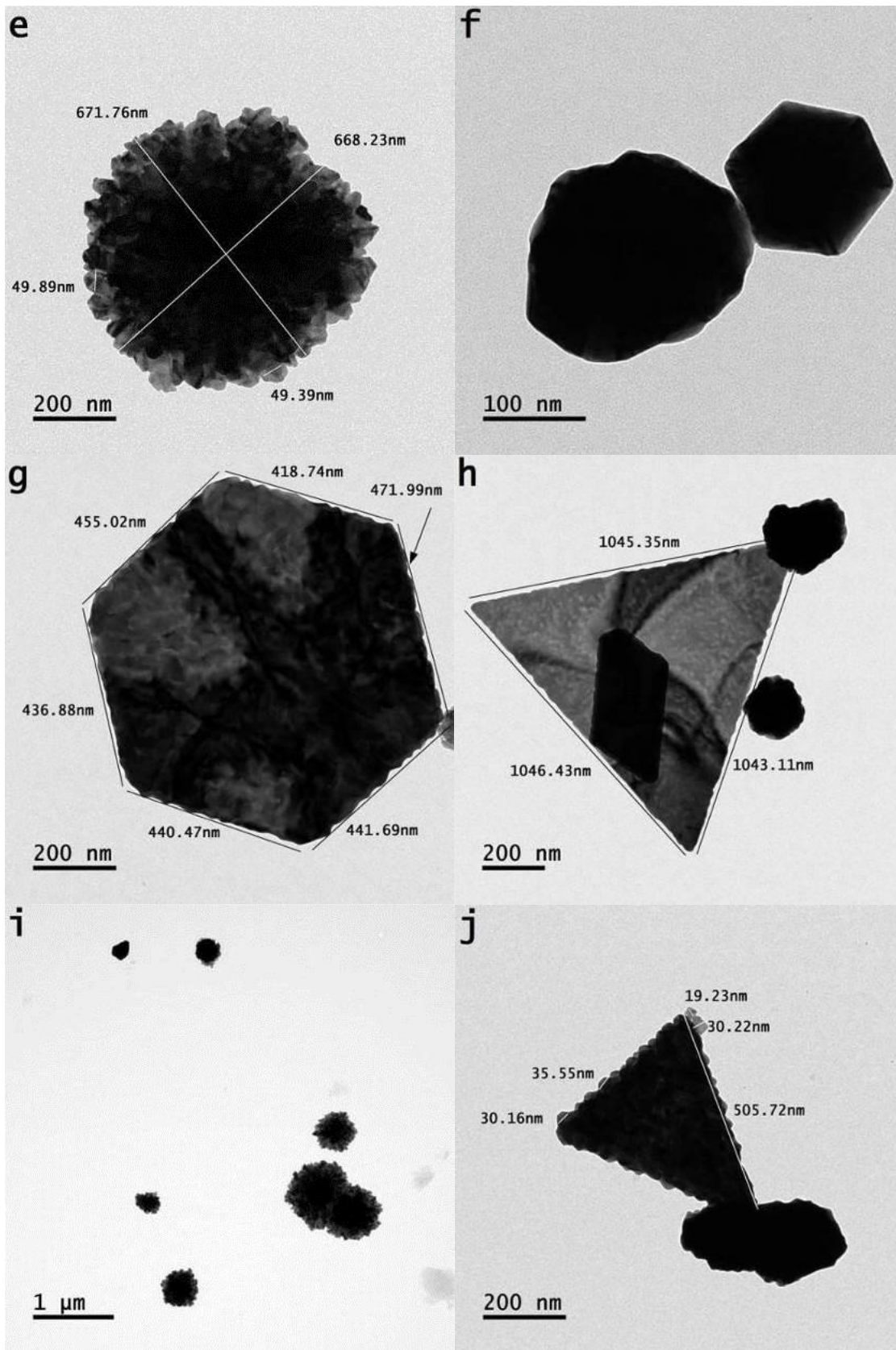


Figure 7: (a-j) Bright field microscope images of particles showing distorted particles (except in 'a')/ SAPR patterns (A-D); precursor concentration 1.20 mM and Argon flow rate 100 sccm

In SAPR patterns of particles, shapes other than rod or bar having distance between parallel printed intensity spots of ~ 0.24 nm are labeled in Figures 5 (A-C), Figure 6 (B) and Figure 7 (A). On the other hand, the distance between parallel printed intensity spots (which are now intensity lines) in the case of rod (or bar)-shaped particles is ~ 0.27 nm as shown in Figure 5 (F) and in Figure 6 (E). A separate study has discussed the cause of obtaining intensity spots of reflected photons in shape-like lines for one-dimensional particles and in shape like dots for multi-dimensional particles [43].

The colors of processed solutions at different molarities of precursor concentration are shown in Figure 8 (left to right: 0.05 mM, 0.10 mM, 0.30 mM, 0.60 mM, 0.90 mM and 1.20 mM). Besides 100 sccm, solutions were also processed at 50 sccm Argon gas flow rate and their colors are shown in Figure 9 (left to right: 0.07 mM, 0.10 mM, 0.30 mM and 0.60 mM). A different color of each solution is related to the overall size and shape of particles along with their quantity, where mode of travelling light having no more constituents of dust/gaseous atoms determine the nature of its certain originating color. Appearance of distinctive color of a colloidal solution processed at different molar concentration is related to the scheme of processed inter-state electron gaps of elongated atoms (forming structures of smooth elements) of different shapes particles and the number of their overall quantity. These require further investigations.

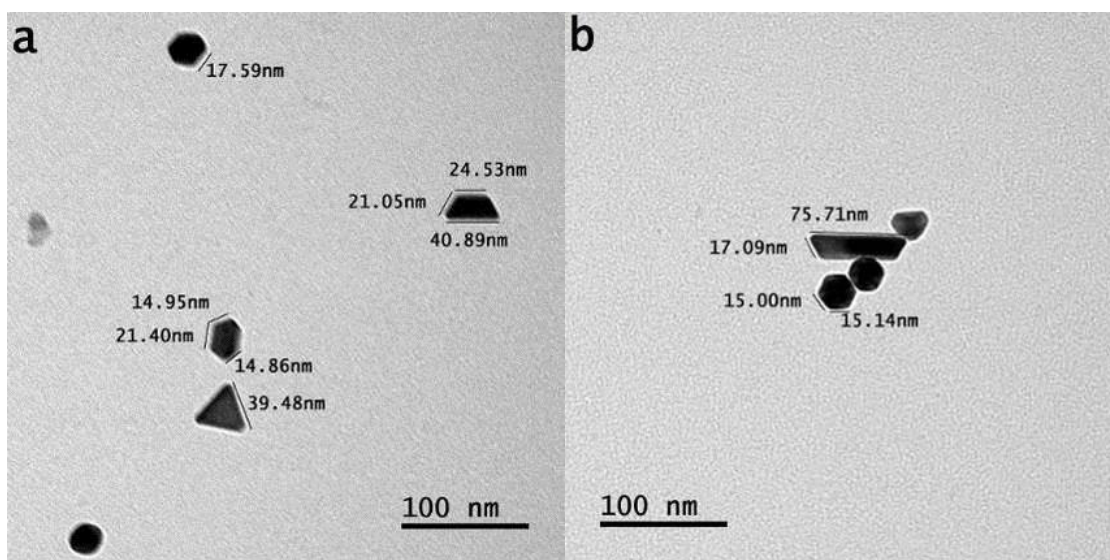


Figure 8: Different color of solutions processed under different molar concentration of precursor (0.05 mM, 0.10 mM, 0.30 mM, 0.60 mM, 0.90 mM and 1.20 mM, left to right) and Argon flow rate 100 sccm



Figure 9: Different color of solutions processed under different molar concentration of precursor (0.07 mM, 0.10 mM, 0.30 mM and 0.60 mM, left to right) and Argon flow rate 50 sccm

The bright field transmission microscope images of their nanoparticles and particles are shown in Figures 10-13. Distorted particles as well as geometric anisotropic particles developed at 50 sccm show identical features to the ones developed at 100 sccm. The nanoparticles/particles developed at different concentrations of gold solution when processed at 50 sccm Argon gas flow rate retain their shapes as in the case of nanoparticles/particles developed at 100 sccm Argon gas flow rate. Many of the nanoparticles developed in their anisotropic shapes at precursor concentration 0.07 mM as shown in Figure 10 (a-c), in different bright field transmission microscope images.



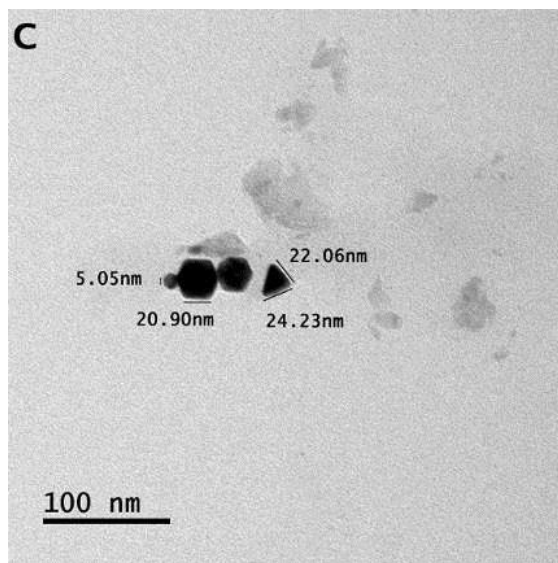
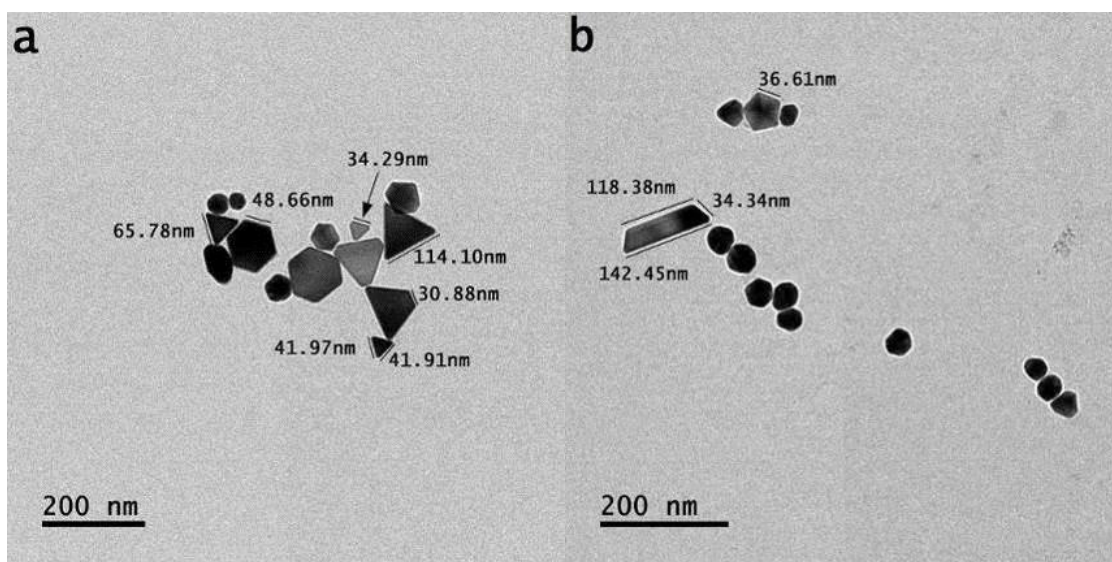


Figure 10: Bright field transmission microscope images of nanoparticles showing both geometric anisotropic and distorted shapes; precursor concentration 0.07 mM and Argon flow rate 50 sccm

The quantity of nanoparticles/particles having anisotropic shapes is further increased at precursor concentration 0.10 mM. As shown in Figure 11 (a-d), there are many nanoparticles/particles which are developed in anisotropic shapes. Nanoparticles of very small-size and very large-size are found in a large number as shown in Figure 11 (a) and Figure 11 (c).



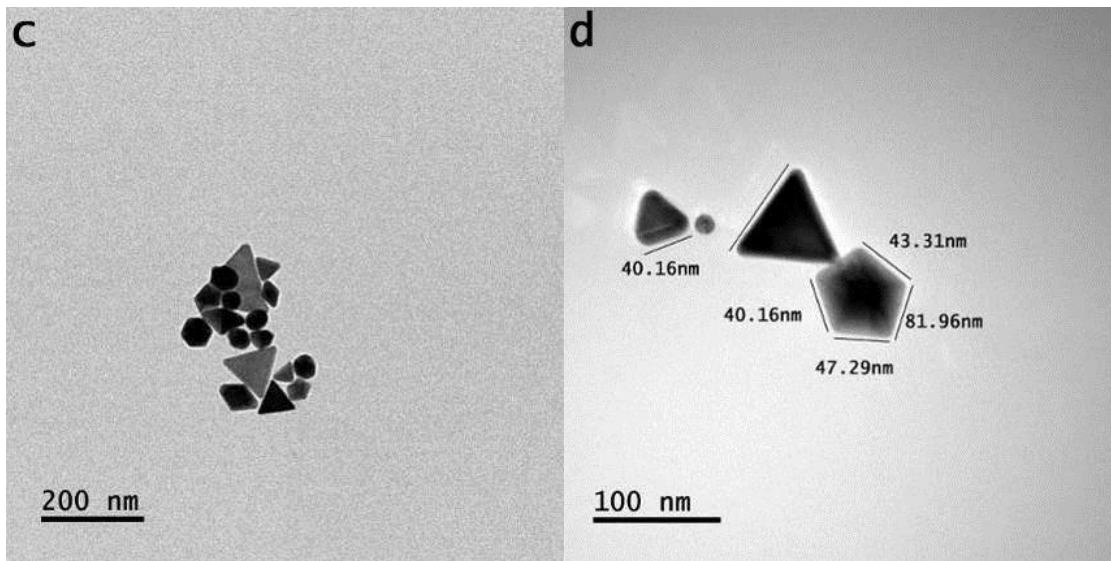
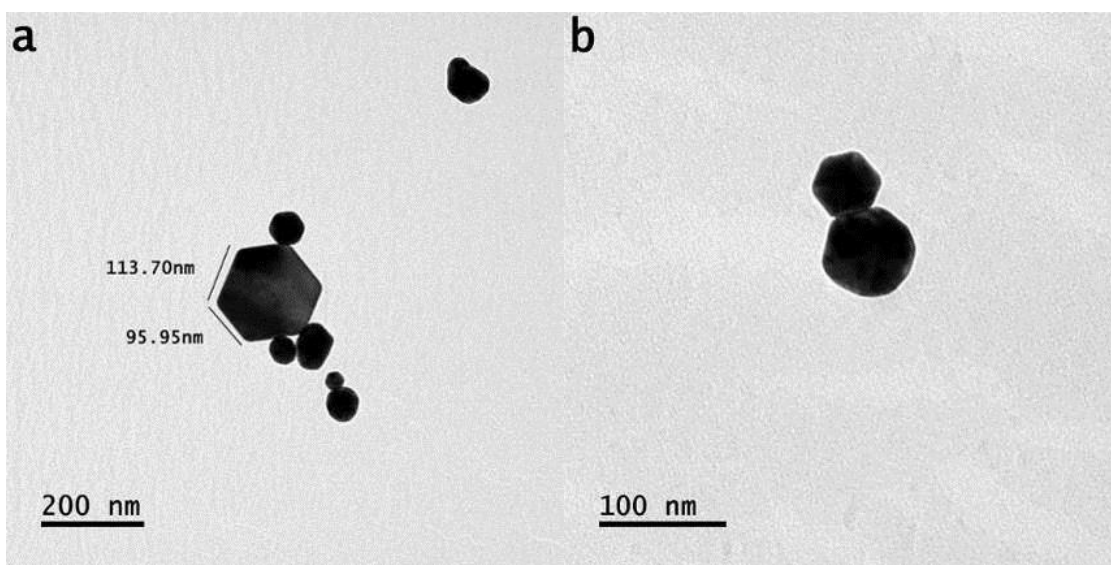


Figure 11: Bright field transmission microscope images of nanoparticles showing both geometric anisotropic and distorted shapes; precursor concentration 0.10 mM and Argon flow rate 50 sccm

The size of nanoparticles/particles is increased further when higher concentration of gold solution is processed where both anisotropic and distorted shapes of the particles are developed as shown in Figure 12 (a-c). Distorted nanoparticles and particles assembled to an anisotropic particle to fill the vacant space through available forces as shown in Figure 12 (a). Both distorted nanoparticles and particles also assembled to fill their vacant regions under the mixed-behaviors of conceivably available forces as shown in Figure 12 (c).



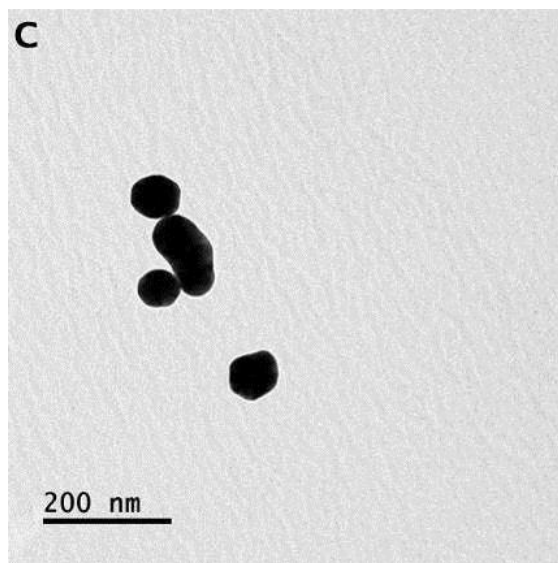
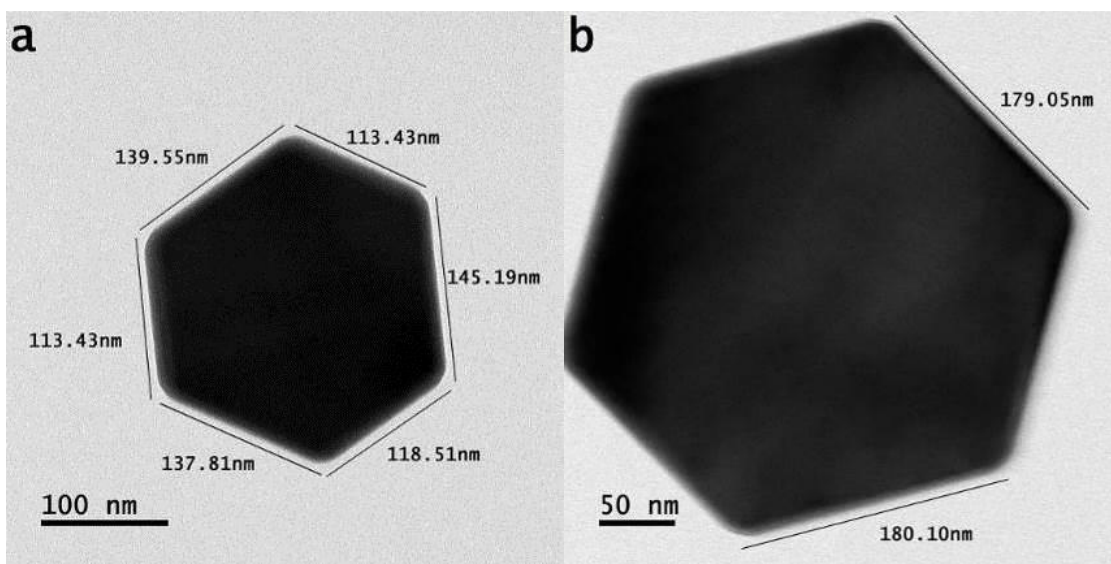


Figure 12: Bright field transmission microscope images of nanoparticles/particles showing both anisotropic and distorted shapes; precursor concentration 0.30 mM and Argon flow rate 50 sccm

Different bright-field transmission microscope images of nanoparticles/particles developed at 50 sccm Argon gas flow rate when the precursor concentration was 0.60 mM are shown in Figure 13. Some of the nanoparticles/particles are developed in the lengths of their sides having precision of an atom, or few atoms, for example, a triangle-shaped particle shown in Figure 13 (g). The different hexagon-shaped nanoparticles (or particles) shown in Figure 13 (c) also indicate the lengths of their sides in highly-controlled precision.



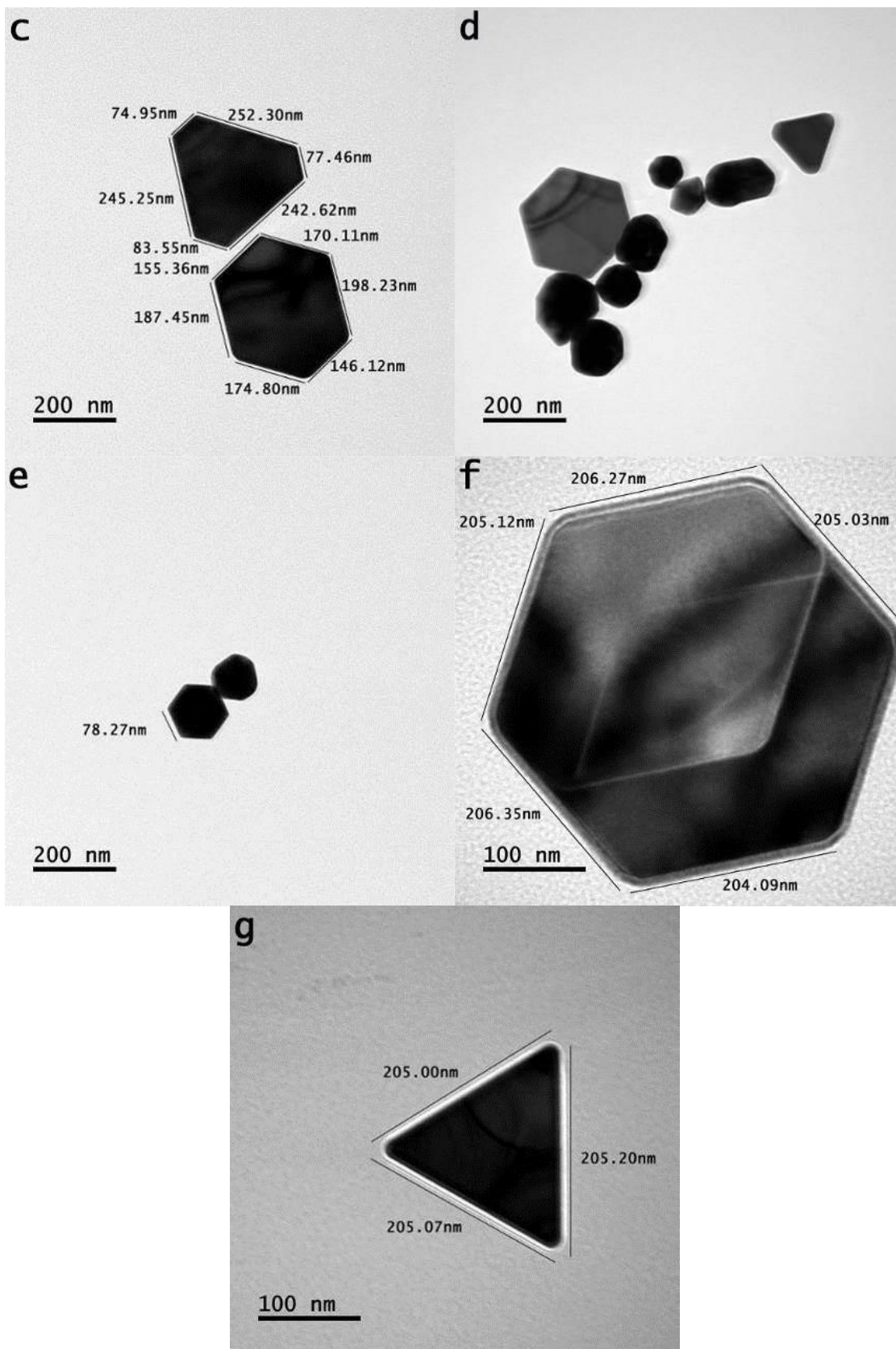


Figure 13: Bright field transmission microscope images of particles showing both geometric anisotropic and distorted shapes; precursor concentration 0.60 mM and Argon gas flow rate 50 sccm

Several different shapes of nanoparticles and particles are shown in Figure 14 (a). A triangle-shaped nanoparticle encircled in Figure 14 (a) was dealt with high-resolution transmission microscope image as in Figure 14 (b) where width of elongated atoms of one-dimensional arrays forming a structure of smooth element is ~ 0.12 nm. A structure of smooth element develops when atoms of one-dimensional array bind through their elongation (at equal rate from both sides of their centers) while exerting the force along opposite poles in the surface-format [34]. So, structures of smooth elements are mainly related to tiny particles having their triangular shapes. An elongation behavior of single gold atom is discussed under the equal rate to both sides (poles) from its center [31]. In the elongation behavior of an atom, electrons of both sides from its (atom) center orientate from the lateral-orientation to the adjacent-orientation [39].

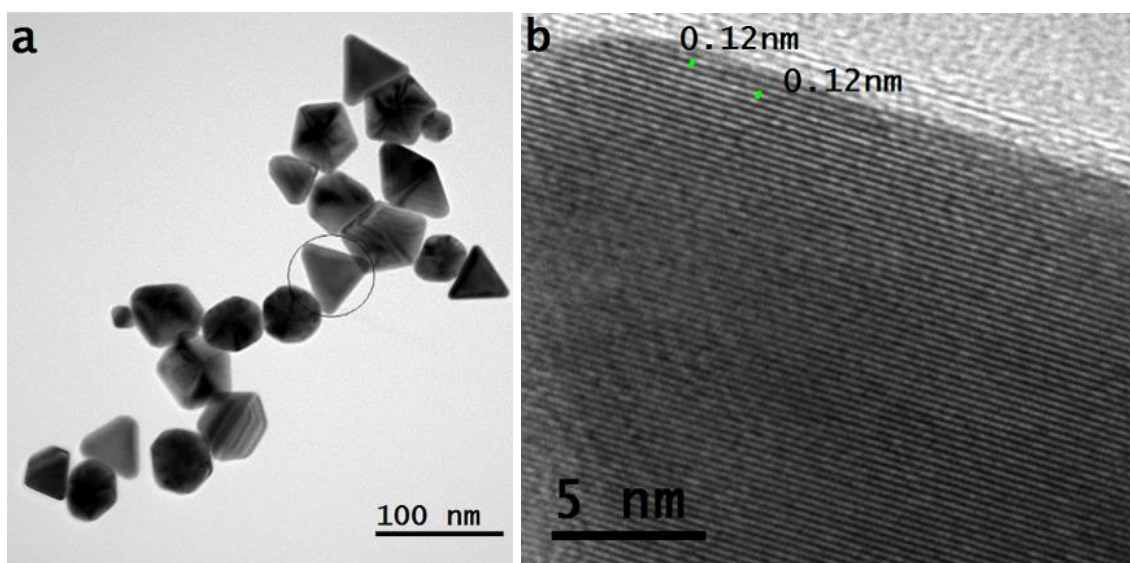


Figure 14: (a) bright field transmission microscope image of nanoparticles showing both geometric anisotropic and distorted shapes at 0.10 mM and (b) magnified high-resolution transmission microscope image taken from the encircled triangle in 'a' shows equal width of structure of smooth element and inter-spacing distance (approx.); precursor concentration 0.10 mM and Argon gas flow rate 50 sccm

Nanoparticles/particles that gets synthesized at Argon gas flow rate of 50 sccm show intensive contrast in terms of dark color as compared to different-featured nanoparticles/particles synthesized at Argon gas flow rate of 100 sccm. This is more

relevant to elongation behavior of atoms in different tiny-shaped particles developing nanoparticles/particles of featured anisotropic shapes. At Argon gas flow rate of 50 sccm, elongation rate of gold atoms is slightly less (at sub-angstrom level) due to lower concentration of flowing Argon gas. Therefore, splitted electron streams of flowing inert gas atoms (under lower concentration) impinge to the underneath matter (gold atoms) at a lower rate. However, due to the entrance of less population (density) of photons and electron streams (resulted under splitted flowing inert gas atoms) in the solution, the average size of nanoparticles/particles also becomes smaller as compared to those developed for 100 sccm Argon gas flow rate. Under different Argon gas flow rate, it is expected that inter-state electron gaps of elongated atoms of structures of smooth elements of nanoparticles/particles is varied at sub-angstrom ($\leq 0.10 \text{ \AA}$) level along with their sizes. It is observable in the bright field transmission microscope images of nanoparticles/particles that get developed at 50 sccm and 100 sccm Argon gas flow rates that they reveal not only a bit difference in the size, but also solutions with different colors. So, by varying the inter-state electron gaps of elongated gold atoms (or by atoms of other suitable elements), it is possible to originate the underlying science of different colors. However, a detailed study is required to investigate the influence of different Argon flow rate on the structure and, ultimately, on their shape and size also. This will possibly depict the overall picture of splitting light into different colors through different colloidal matters processed under different conditions.

Packing trends of tiny-shaped particles (under force existing in surface-format) can be depicted from their differently-developed geometric anisotropic particles. Assembling angles can be extracted from the distributed intensity spots in SAPR patterns of their particles. In Figure 6 (C), SAPR pattern indicates that spotted spots reflected at the front-surfaces are under their certain pace where photons (not electrons) reflected from the structures of smooth elements of above-positioned particle (hexagon-shaped particle) as well as the underneath one (hexagon-shaped particle); in the case of latter, photons reflected at the surface of underlying structure while entering through the inter-spacing distance of structures of smooth elements of above-positioned particle. Each structure of smooth element is related to the elongated atoms of one-dimensional array.

On amalgamation of atoms at set precursor concentration, they are developed in different tiny-sized particles under the application of packets of nano-energy. At the lowest concentration of precursor (0.05 mM), very few gold atoms were available, which get uplifted to the solution surface, but the packet of each nano-energy possesses the same size and shape under set tuned ratio of pulse OFF to ON time as given in the section of experimental details. The atoms underneath packets of nano-energy are insufficient to deal an average size of tiny particle ~ 1.3 nm with no specific geometry of shape. This is because of their not having the ability to form precise compact uniform monolayer assembly at air-solution interface. Thus, at 0.05 mM (and when unity ratio of pulse OFF to ON time), atoms do not develop their tiny particles in a triangular-shape (Figure 15a₁). Because atoms do not form one-dimensional arrays of their tiny clusters, thus, they do not elongate for developing structures of smooth elements as shown in Figure 15 (a₂). They get packed under the exertion of force having mixed-behaviors resulting into less-distorted or sphere-shaped nanoparticle as shown in Figure 15 (a₃).

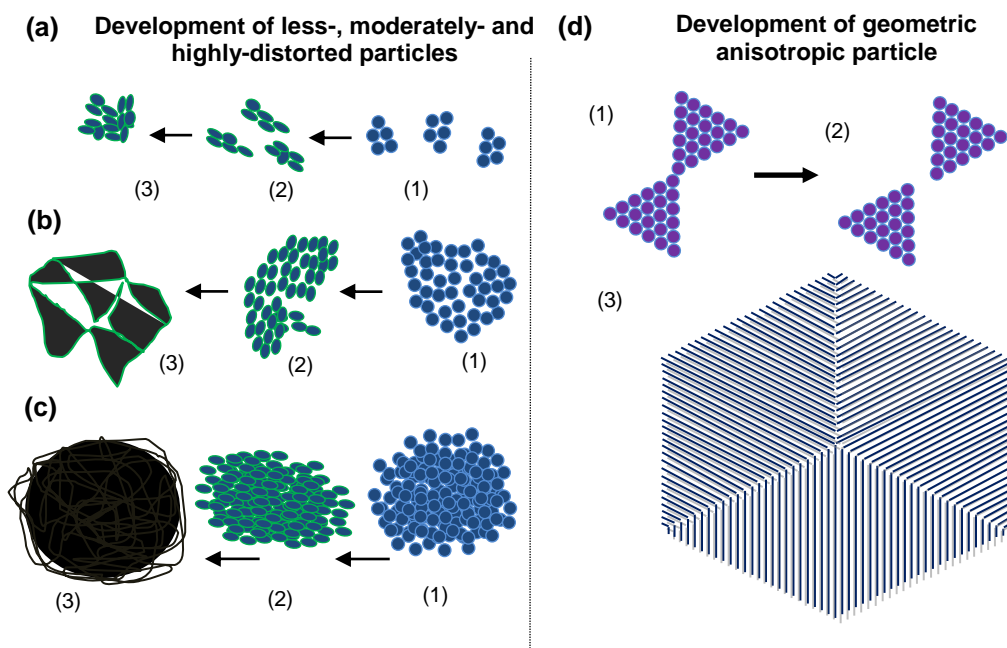


Figure 15: (a₁) less-disordered tiny particles, (a₂) deformation of atoms of 'less-disordered tiny particles', (a₃) less-distorted particle; (b₁) moderately-disordered tiny particle, (b₂) deformation of atoms of 'moderately-disordered tiny particle', (b₃) partially-distorted particle; (c₁) highly-disordered tiny particle, (c₂) deformation of atoms of 'highly-disordered tiny particle', (c₃) highly-distorted particle; (d₁) tiny particle of a joined triangular-shape, (d₂) separated tiny particle into two equal triangle-shaped tiny particles and (d₃)

hexagon-shaped particle having the multi (six)-dimensional shape where the same structure of elongated atoms for each dimension (face) is observed

At fixed bipolar pulse ON/OFF time, increasing the precursor concentration from ~ 0.07 mM to ~ 0.90 mM, many tiny particles get developed in a triangular-shape where their size is increased on increasing the precursor concentration. However, for intermediate precursor concentrations (~ 0.07 mM to ~ 0.90 mM), tiny-sized particles were also developed in a non-triangular-shape (and in more number in certain regions of solution), they are termed as moderately-disordered tiny particle as shown in Figure 15 (b₁). Such tiny particles do not deal packing under exerting force of a uniform manner. Thus, atoms of such tiny particle didn't elongate uniformly as sketched in Figure 15 (b₂) and termed as moderately-distorted tiny particle. So, such tiny particles packed under exertion of forces having not consistent behavior of theirs. This results into the development of distorted particles as shown in Figure 15 (b₃).

At 1.20 mM, precursor concentration is very large, and assembly developed at solution surface doesn't deal the compactness in gold atoms from the start of starting the process. Due to the uplifting of much higher amount of gold atoms to solution surface, it has resulted into the development of an assembly of disorderness instead of monolayer. But, the packets of nano-energy contained the same size and shape for binding atoms as in the case of processing solutions of lower concentration. Therefore, at initial stage of the process, all the tiny-sized particles get developed are highly-disordered as they are large enough in their size. The highly-disordered tiny particles do not get develop in a triangular-shape, so, their structures do not undertake one-dimensional arrays of atoms. A highly-disordered tiny particle is shown in Figure 15 (c₁) where groups of atoms (total atoms: 171) configured along the different sides. Thus, atoms of highly-disordered tiny particle get elongated along different sides where forces were exerted along the poles of multi-orientated electrons (so, they are in non-uniform manner), which is termed as highly-distorted tiny particle as shown in Figure 15 (c₂). Such large size tiny particles do not get packed under the exertion of force having a uniform impact. The packing and assembling of such highly-distorted tiny particles resulted into the development of a highly-distorted particle as shown in Figure 15 (c₃).

A joined triangular-shape tiny particle is shown in Figure 15 (d₁), which was developed under the application of bipolar pulse while processing the solution of gold under certain precursor concentration. The joined triangular-shape tiny particles separated at the point of connection under the exertion of force along opposite poles as shown in Figure 15 (d₂). Six such tiny particles arriving from the different regions of solution surface located at a point nearly equidistant to the center of their packing nucleated the mono-layer of hexagon-shaped particle (at the center of pulse-based electron-photon-solution interface). Packing of several such tiny-shaped particles while retaining intact initially originated the symmetry resulting into the development of hexagon-shaped particle as shown in Figure 15 (d₃). Here, the width of each structure of smooth element along with their inter-spacing distance has remained almost the same as in the case of particle shown in Figure 14 (b). In Figure 14 (b), both width and inter-spacing distance are measured with original scale marker. Thickness of each structure of smooth element has appeared to be the same as that of the resultant width of each elongated one-dimensional array of gold atoms (~ 0.12 nm). A structure of smooth element is related to elongated atoms of one-dimensional array when they were in the certain transition state [34]. A further detail of developing various geometric anisotropic particles is given elsewhere [40].

Under very high concentration of gold precursor (1.20 mM), average size of tiny particles was 50 nm at the start of process and, on prolonging the process time, tiny particles resulted in a decreased size as discussed elsewhere [30]. Therefore, the geometric anisotropic particle shown in Figure 7 (a) is due to the smaller size tiny particles developed at the later stage of the process. This indicates that, by increasing the process duration, the favorable conditions prevailed. The tiny particles of a non-triangular-shape have been turned into a triangular-shape under the favorable conditions of the process. Therefore, initial concentration of precursor is not the only parameter controlling the size and shape of tiny particles. Size and shape of tiny particles as well as nanoparticles/particles depend on time-to-time change in the precursor concentration also.

Simultaneous assembling of structures of smooth elements of two triangle-shaped tiny particles at the center of light-glow from opposite sides is along nearly the same

axis, so, they are developing a mono-layer of developing rod- or bar-shaped 1-D particle. A pentagon-shaped particle and a hexagon-shaped particle are related to five-dimension and six-dimension, respectively. However, such dimensional shapes are not possible when gold atoms result in the evolution of structure in the original format by executing confined inter-state electron-dynamics [33]. So, developing such types of large-shaped particles dealing anisotropy, which are also the part of extensive debate in the literature, is under the development of tiny-shaped particles first but not straightforwardly through the binding mechanism of neutral state gold atoms into their grounded-format.

An approx. percentage of both anisotropic particles and distorted particles developed at different molar concentrations of gold precursor are drawn in chart-shape as shown in the Figure 16.

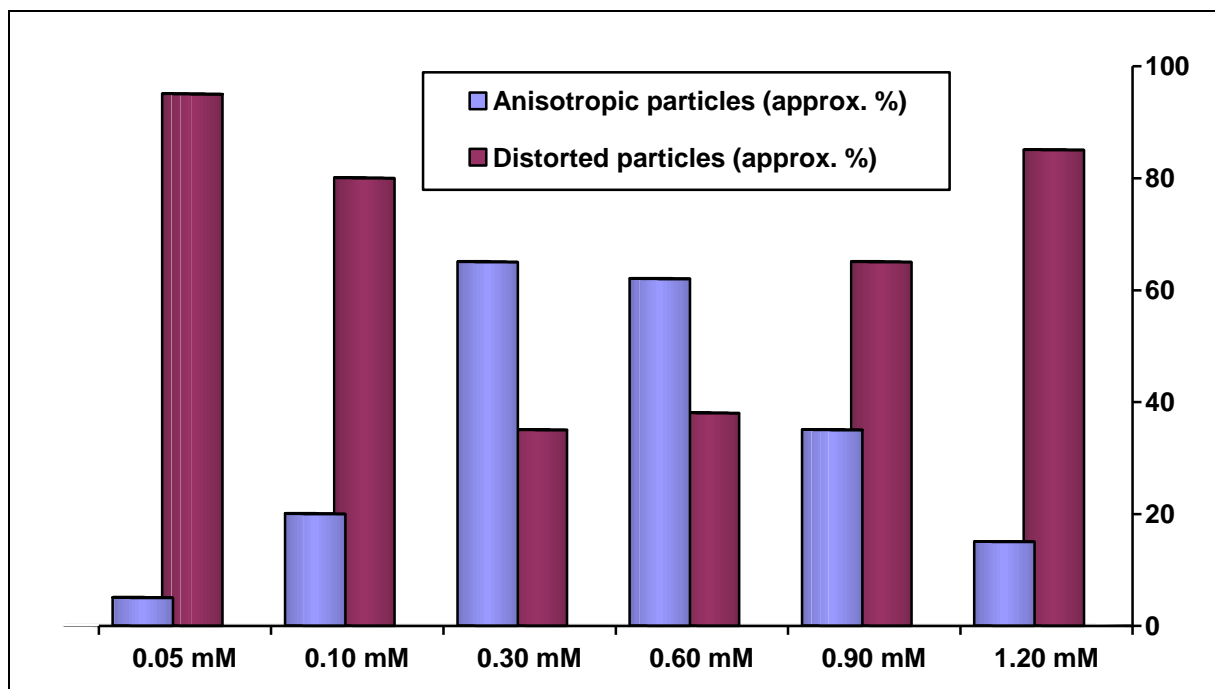


Figure 16: Approx. %age of anisotropic and distorted particles developed at different molar concentrations of gold precursor while employing pulse-based electron-photon-solution interface process when fixed duration in each process was 10 minutes and bipolar pulse ON/OFF time was 10 μ sec

Origin of gas- and solid -natured atoms has been discussed elsewhere [41]. As per nature of atoms of tiny-sized particles, they can be a defective nanomedicine instead of being an effective one [42]. Gold shapes of one-dimension and multi-dimension clearly identify the role of forces at ground surface (in surface-format) [43]. Developing hard

coating is nearly under the switched force-energy behaviors of gas- and solid-natured atoms [44]. It has been pointed out that upto certain numbers of atoms, tiny particles are developed in hcp structures [45] and tiny particle size upto a point shows metallic character [46]. It has been stated that besides geometry and entropy, in-progress research efforts should also consider the dynamics in addition to structure [47] and disordered jammed configuration is not the only one in any known protocol but there are also ordered metrics, which characterize the order of packing [48]. A study on size-controlled gold nanoparticles while synthesizing in photochemical process has been given elsewhere [49]. From the application point of view, nanoparticles and particles having distorted shapes show potential in various catalytic applications, whereas, those in geometric anisotropic shapes indicate a potential to use them as ultra-high-speed devices along with applications in diversified areas, in optics, medical and photonic devices, etc.

4. Conclusions

In custom-built pulse-based electron-photon-solution interface process, the development of geometric anisotropic gold particles is due to the packing of triangle-shaped tiny particles where their structures of smooth elements get assembled under the controlled orientations at electron-levels. Tiny-shaped particles arrive from the different regions of solution surface to assemble their structures of smooth elements at center of light-glow. Developing of distorted particles is under the coalescences of non-triangular-shape tiny particles where they do not necessarily coalesce at center of light-glow. The development of tiny particles in different sizes depend on the initial amount of precursor concentration. A certain amount of precursor concentration under the fixed ratio of bipolar pulse OFF to ON time results into the development of many tiny particles having a triangular-shape. Increasing the molar concentration of gold precursor from 0.05 mM to 1.20 mM, average size of gold tiny particles increases from 1.3 nm (approx.) to 50 nm (approx.). At 0.05 mM, tiny-sized particles do not develop in a triangular-shape. Packing of such tiny particles results into the development of less-distorted sphere-shaped nanoparticles. At 0.07 to 0.90 mM, many tiny-sized particles get developed in a triangular-shape, but they get developed in maximum amount (number)

at precursor concentration 0.30 mM and 0.60 mM. At 1.20 mM, many tiny-sized particles do not get developed in a triangular-shape and their packing results into develop distorted particles. The SAPR patterns of distorted particles reveal their structure in the disorderness. The decreasing Argon gas flow rate from 100 sccm to 50 sccm doesn't influence the overall mechanism of developing of particles' shape but may influence the electronic structure of elongated atoms in the decimal range of an angstrom, thus, forming structures of smooth elements. The color of the processed solution for each molar concentration of gold changes due to overall impact of the incident light. The modified inter-state electron gaps of elongated atoms forming structures of smooth elements having certain shapes become the main cause of appeared distinctive color of filtered-light while leaving different-shaped particles under the impactful scale of an angle.

Acknowledgements:

Mubarak Ali thanks National Science Council (now MOST) Taiwan (R.O.C.) for awarding postdoctorship: NSC-102-2811-M-032-008 (August 2013- July 2014). Authors wish to thank Dr. Kamatchi Jothiramalingam Sankaran, National Tsing Hua University and Mr. Vic Chen, Tamkang University, Taiwan (R.O.C.) for assisting in TEM operation.

References:

1. Daniel, M-C, Astruc D (2004) Gold Nanoparticles: Assembly, Supramolecular Chemistry, Quantum-Size-Related Properties, and Applications toward Biology, Catalysis, and Nanotechnology. *Chem. Rev.* 104; 293-346.
2. Brust M, Walker M, Bethell D, Schiffrin D J, Whyman R (1994) Synthesis of Thiol-derivatised Gold Nanoparticles in a Two-phase Liquid-Liquid System. *J. Chem. Soc., Chem. Commun.* 801-802.
3. Whetten RL; Khoury JT, Alvarez MM, Murthy S, Vezmar I, Wang ZL, Stephens PW, Cleveland, CL, Luedtke WD, Landman U (1996) Nanocrystal Gold Molecules. *Adv. Mater.* 8; 428-433.

4. Link, S, El-Sayed, MA (2000) Shape and size dependence of radiative, nonradiative and photothermal properties of gold nanocrystals. *Inter. Rev. Phys. Chem.* 19; 409-453.
5. Brown LO, Hutchison JE (2001) Formation and Electron Diffraction Studies of Ordered 2-D and 3-D Superlattices of Amine-Stabilized Gold Nanocrystals. *J. Phys. Chem. B* 105;8911-8916.
6. Whitesides GM, Boncheva M (2002) Beyond molecules: Self-assembly of mesoscopic and macroscopic components. *Proc. Natl. Acad. Sci. U.S.A.* 99; 4769-4774.
7. Brust M, Kiely CJ (2002) Some recent advances in nanostructure preparation from gold and silver particles: a short topical review. *Colloids and Surfaces A: Physicochem. Eng. Aspects* 202; 175-186.
8. Huang J, Kim F, Tao AR, Connor S, Yang P (2005) Spontaneous formation of nanoparticle stripe patterns through dewetting. *Nat. Mater.* 4; 896-900.
9. Glotzer SC, Horsch MA, Iacovella CR, Zhang Z, Chan ER, Zhang X (2005) Self-assembly of anisotropic tethered nanoparticle shape amphiphiles. *Curr. Opin. Colloid Interface Sci.* 10;287-295.
10. Glotzer SC, Solomon MJ (2007) Anisotropy of building blocks and their assembly into complex structures. *Nature Mater.* 6; 557-562.
11. Shaw CP, Fernig DG, Lévy R (2011) Gold nanoparticles as advanced building blocks for nanoscale self-assembled systems. *J. Mater. Chem.* 21; 12181-12187.
12. Vanmaekelbergh D (2011) Self-assembly of colloidal nanocrystals as route to novel classes of nanostructured materials. *Nano Today* 6;419-437.
13. Liu N, Tang ML, Hentschel M, Giessen H, Alivisatos AP (2011) Nanoantenna-enhanced gas sensing in a single tailored nanofocus. *Nat. Mater.* 10; 631-637.
14. Mulvaney P (1996) Surface Plasmon Spectroscopy of Nanosized Metal Particles. *Langmuir* 12: 788-800.
15. Lofton C, Sigmund W (2005) Mechanisms controlling crystal habits of gold and silver colloids. *Adv. Funct. Mater.* 15; 1197-1208.
16. Tao A, Sinsermsuksakul P, Yang P (2006) Polyhedral Silver Nanocrystals with Distinct Scattering Signatures. *Angew. Chem. Int. Ed.* 45; 4597-4601.

17. Millstone JE, Hurst SJ, Métraux GS, Cutler JI, Mirkin CA (2009) Colloidal Gold and Silver Triangular Nanoprisms. *Small* 5; 646-664.
18. Mariotti D, Patel J, Švrček V, Maguire P (2012) Plasma –Liquid Interactions at Atmospheric Pressure for Nanomaterials Synthesis and Surface Engineering. *Plasma Process. Polym.* 9; 1074-1085.
19. Patel J, Němčová L, Maguire P, Graham WG, Mariotti D (2013) Synthesis of surfactant-free electrostatically stabilized gold nanoparticles by plasma –induced liquid Chemistry. *Nanotechnology* 24;245604-14.
20. Huang X, Li Y, Zhong X (2014) Effect of experimental conditions on size control of Au nanoparticles synthesized by atmospheric microplasma electrochemistry. *Nanoscale Research Lett.* 9; 572-578.
21. Saito N, Hieda J, Takai O (2009) Synthesis process of gold nanoparticles in solution plasma. *Thin Solid Films* 518; 912-917.
22. Furuya K, Hirowatari Y, Ishioka T, Harata A (2007) Protective Agent-free Preparation of Gold Nanoplates and Nanorods in Aqueous H₂AuCl₄ Solutions Using Gas–Liquid Interface Discharge. *Chem. Lett.* 36; 1088-1089.
23. Hieda J, Saito N, Takai O (2008) Exotic shapes of gold nanoparticles synthesized using plasma in aqueous solution. *J. Vac. Sci. Technol. A* 26;854-856.
24. Shirai N, Uchida S, Tochikubo F (2014) Synthesis of metal nanoparticles by dual plasma electrolysis using atmospheric dc glow discharge in contact with liquid. *Jpn. J. Appl. Phys.* 53; 046202-07.
25. Baba K, Kaneko T, Hatakeyama R (2009) Efficient Synthesis of Gold Nanoparticles Using Ion Irradiation in Gas–Liquid Interfacial Plasmas. *Appl. Phys. Exp.* 2;035006-08.
26. Liu Y, Zhang X (2011) Metamaterials: a new frontier of science and technology. *Chem. Soc. Rev.* 40; 2494-2507.
27. Kuzyk A, et al. (2012) DNA-based self-assembly of chiral plasmonic nanostructures with tailored optical response. *Nature* 483; 311-314.
28. Kim J, Lee Y, Sun S (2010) Structurally ordered FePt nanoparticles and their enhanced catalysis for oxygen reduction reaction. *J. Am. Chem. Soc.* 132; 4996-4997.

29. Kusada K, et al. (2013) Discovery of face-centered-cubic ruthenium nanoparticles: facile size-controlled synthesis using the chemical reduction method. *J. Am. Chem. Soc.* 135; 5493-5496.
30. Ali, M., Lin, I –N. The effect of the Electronic Structure, Phase Transition and Localized Dynamics of Atoms in the formation of Tiny Particles of Gold. <http://arxiv.org/abs/1604.07144v10>
31. Ali M. Atoms of electron transition deform or elongate but do not ionize while inert gas atoms split under photonic current instead of electric. <http://arxiv.org/abs/1611.05392v15>
32. Ali M. Revealing the Phenomena of Heat and Photon Energy on Dealing Matter at Atomic level. <http://www.preprints.org/manuscript/201701.0028/v10>
33. Ali M. Structure evolution in atoms of solid-state dealing electron transitions under confined inter-state electron-dynamics. <http://arxiv.org/abs/1611.01255v16>
34. Ali M. The study of tiny-shaped particles developing mono-layer dealing localized gravity at solution surface. <http://arxiv.org/abs/1609.08047v16>
35. Ali M, Lin I –N. Phase transitions and critical phenomena of tiny grains carbon films synthesized in microwave-based vapor deposition system. *Surf. Interface Anal.* 2018;1–11. <https://doi.org/10.1002/sia.6593>
36. Ali M, Ürgen M (2017) Switching dynamics of morphology-structure in chemically deposited carbon films-a new insight. *Carbon*, 122; 653-663.
37. Ali M, Lin, I –N, Yeh, C -Y. Tapping Opportunity of Tiny-Shaped Particles and Role of Precursor in Developing Shaped Particles. *NANO* 13 (7) (2018) 1850073 (16 pages).
38. Ali M, Lin, I –N. Controlling morphology-structure of particles at different pulse rate, polarity and effect of photons on structure. <http://arxiv.org/abs/1605.04408v13>
39. Ali M, Lin, I –N. Formation of tiny particles and their extended shapes: origin of physics and chemistry of materials. *Appl. Nanosci.* 9 (2019) <https://doi.org/10.1007/s13204-018-0937-z>
40. Ali, M, Lin, I –N, Yeh, C –J. Predictor Packing in Developing Unprecedented Shaped Colloidal Particles. *NANO* 13 (9) (2018) 1850109 (15 pages).

41. Ali, M. Why Atoms of Some Elements are in Gas State and Some in Solid State, but Carbon Works on Either Side. <https://www.researchgate.net/publication/323723379>
42. Ali, M. (2018) Nanoparticles-Photons: Effective or Defective Nanomedicine. *J. Nanomed. Res.* 5(6); 241-243.
43. Ali, M, Lin, I –N, Precise Structural Identification of High Aspect Ratios Gold Particles Developed by Unprecedented Machinic Approach. <https://www.researchgate.net/publication/329066950>
44. Ali, M, Hamzah, E, Toff, M R M. Hard Coating is Because of Oppositely Worked Force-Energy Behaviors of Atoms. <https://www.preprints.org/manuscript/201802.0040/v8>
45. Negishi Y, et al. (2015) A Critical Size for Emergence of Nonbulk Electronic and Geometric Structures in Dodecanethiolate-Protected Au Clusters. *J. Am. Chem. Soc.* 137; 1206-1212.
46. Moscatelli A (2015) Gold nanoparticles: Metallic up to a point. *Nature Nanotechnol.* DOI:10.1038/nnano.2015.16.
47. Manoharan, V N (2015) Colloidal matter: Packing, geometry, and entropy, *Science* 349; 1253751.
48. Atkinson S, Stillinger, F H, Torquato S (2015) Existence of isostatic, maximally random jammed monodisperse hard-disk packings, *Proc. Natl. Acad. Sci. U.S.A.* 111; 18436-18441.
49. Kim, J -H, Lavin, B W, Burnett, R D, Boote, B W (2011) Controlled synthesis of gold nanoparticles by fluorescent light irradiation, *Nanotechnology* 22; 285602.